Aus dem Max-Delbrück-Centrum für Molekulare Medizin
Cellular Neuroscience

DISSERTATION

E-NTPDase 1 modulation of neuronal and astrocytic activity in the CNS

zur Erlangung des akademischen Grades
Doctor of Philosophy (PhD)
im Rahmen des
International Graduate Program Medical Neurosciences

vorgelegt der Medizinischen Fakultät
Charité - Universitätsmedizin Berlin

von

Adriana Rocha

aus Loureiro, Portugal

Datum der Promotion: 22.06.2014

For my grandmother

For my aunt

For my mother

For the women of my family,

who are themselves an example of strength and perseverance

I. Contents

II. List of figures

III. List of tables

IV. Abbreviations

°C	Degree Celsius
%	Percent
µA	Microampere
µL	Microlitre
µm	Micrometre
μm^2	Square micrometre
µmol	Micromole
AC	Adenylyl cyclase
ACP	Acid phosphatase
ACSF	Artificial Cerebrospinal Fluid
ADP	Adenosine 5'-diphosphate
ALP	Alkaline phosphatase
AMP	Adenosine 5'-monophosphate
ARL 67156	ARL 67156 trisodium salt
ATP	Adenosine 5'-triphosphate
BBB	Blood-Brain Barrier
BCA	Bicinchoninic Acid
BSA	Bovine serum albumin
Ca^{2+}	Calcium
CD39	Ecto-nucleoside triphosphate diphosphohydrolase-1, ENTPDase1
CD73	Ecto-5'-nucleotidase
CNS	Central nervous system
CNTs	Concentrative nucleoside transporters
CO2	Carbon dioxide
CTRL	Control
Cu^{1+}	Cuprous cation
Cu^{2+}	Copper (II) cation
DAG	Diacylglycerol
ddH2O	Double-distilled water
DMEM	Dulbecco's Modified Eagle's Medium
DMSO	Dimethylsulfoxide
DNA	Deoxyribonucleic Acid
dNTP	Deoxyribonucleotide Triphosphate
E-NPP	Ectonucleotide pyrophosphatases/diphosphodiesterase
ENTs	Equilibrative nucleoside transporter
E-NTPDase1	Ecto-nucleoside triphosphate diphosphohydrolase-1, also known as CD39
FCS	Fetal Calf Serum
Fluo-4 AM	Fluo-4 acetoxymethyl ester

g	Relative centrifugal force
GABA	γ-Aminobutyric acid
h	Hour
Half rep	Time for half repolarization
HBSS	Hank's Balanced Salt Solution
Hz	Hertz
I STM	Integral of membrane depolarization over time
$Ins(1,4,5)P_3$	Inositol 1,4,5-trisphosphate
kHz	Kilohertz
Km	Michaelis constant
KO	Knock-out
Mg^{2+}	Magnesium
mg	Milligram
min	Minute
mL	Millilitre
mM	Millimolar
ms	Millisecond
mV	Millivolt
MΩ	Megaohm
nm	Nanometre
NMDA	N-Methyl-D-aspartate
OD	Optical density
P	Postnatal day
pA	Picoampere
PBS	Phosphate-Buffered Saline
PCR	Polymerase chain reaction
Pi	Free phosphate
PLC	Phospholipase C
PPADS	Pyridoxalphosphate-6-azophenyl-2',4'-disulfonic acid tetrasodium salt
Ra	Access resistance
rpm	Revolutions per minute
RT	Room temperature
s	Second
s.e.m.	Standard error of the mean
SDS	Sodium Dodecyl Sulfate
STM depol	Stimulus-evoked depolarization
TAE	Tris-acetate-EDTA buffer
TCA	Trichloroacetic acid
Tris	Tris-(hydroxymethyl)-aminomethane
U	Units

UDP	Uracyl 5’-diphosphate
UV	Ultraviolet
V	Volt
w/v	weight per volume
WT	Wildtype

1. Summary

Purinergic signalling is one of the most important mechanisms of neuron-glia modulation and has an essential role in the maintenance of the CNS. E-NTPDase 1 (also known as CD39) is an enzyme present in microglia which is capable of metabolizing ATP to AMP. Due to the extended ramified morphology of microglia, CD39 can be important in regulating P1 and P2 signalling in nearby neurons and astrocytes.

Using a CD39 $^{-/-}$ mouse, we investigated the effect of CD39 on glial (microglia and astrocytes) and neuronal activity. Initial experiments with phosphate assays showed that CD39 is the only enzyme responsible for extracellular ATP and ADP dephosphorylation in microglia.
Insight into glia-glia signalling (microglia-astrocytes) was acquired via experiments with astrocyte-evoked calcium waves. The calcium wave spread further in the absence of CD39, in a purine-dependent mechanism reversible by PPADS application. Furthermore, the wild type phenotype was restored by apyrase application. There was no significant effect with direct application of ATP or ARL 67156, which prevents ATP metabolization.
Additionally, in CD39 $^{-/-}$ mice, neurons showed an increased degree of excitability, characterized by an increase of spontaneous action potentials during the repolarization phase and a higher frequency of excitatory post-synaptic events. This neuronal excitability could be mimicked by PPADS application, but not by direct application of ATP or ARL 67156.
The failure to mimic the CD39 knock-out phenotype pharmacologically pointed towards deeper changes in the transgenic animal during development, which could be due to long-term adenosine mediated inhibition absent in the knock-out mouse.

Taken together, the data suggest a CD39-mediation of neuronal and astrocytic activities, possibly via microglia, but the mechanism is still unknown.
Considering that CD39 is important for microglia in both physio- and pathophysiological states, the neuronal and astrocytic interactions on a physiological level described in this study will ultimately allow further understanding of pathophysiology and how inflammation can modulate the CNS.

2. Zusammenfassung

Purinerge Signalgebung ist einer der wichtigsten Mechanismen der Neuronen-Glia Interaktion und spielt eine essentielle Rolle für die Aufrechterhaltung des homöostatischen Funktionen des Zentralnervensystems. E-NTPDase 1 (auch bekannt als CD39) ist ein Enzym, welches von Mikroglia exprimiert wird und ATP zu AMP metabolisiert. An den mikroglialen Fortsätzen kann CD39 von Bedeutung sein für die Regulation der P1- und P2-Signalgebung in benachbarten Neuronen und Astrozyten.

Um einen möglichen Effekt von CD39 auf gliale (Mikroglia und Astrozyten betreffend) und neuronale Aktivität zu untersuchen, verwendeten wir eine CD39 $^{-/-}$ Maus. Erste Untersuchungen des Phosphatmetabolismus zeigten, dass CD39 als einziges Enzym für die Dephosphorylierung von extrazellulärem ATP und ADP auf Mikroglia zuständig ist. Um jene Glia-Glia-Kommunikation (zwischen Mikroglia und Astrozyten) genauer zu studieren, untersuchte ich die Ausbreitung von Calciumwellen in Astrozyten. In Abwesenheit von CD39 auf Mikroglia breiteten sich die Calciumwellen, im Vergleich zum Wildtyp, über eine größere Fläche aus. Ich konnte zeigen, dass dieser Mechanismus purinabhängig und durch PPADS reversibel ist. Durch Zugabe von Apyrase zu Knockoutschnitten konnte ich einen Effekt ähnlich den Wildtypschnitten beobachten. Weder die Applikation von ATP noch von ARL 67156 (Blocker der ATP-Spaltung) führte zu einem signifikanten Unterschied. Des Weiteren zeigten Neurone der CD39$^{-/-}$ Maus eine erhöhte Erregbarkeit, charakterisiert durch eine gesteigerte Anzahl an spontanen Aktionspotentialen während der Repolarisationsphase und durch eine zunehmende Häufigkeit der exzitatorischen postsynaptischen Potentiale. Diese neuronale Erregbarkeit konnte durch Applikation von PPADS nachgeahmt werden, aber nicht durch Zugabe von ATP oder ARL 67156.
Die Beobachtung, dass der CD39 Knockout-Phänotyp nicht pharmakologisch nachgeahmt werden kann, weist auf mögliche Veränderungen während der Entwicklung hin. Dies geschieht möglicherweise durch langzeitige adenosinvermittelte Inhibition, die der Knockoutmaus fehlt.

Zusammenfassend deuten die von mir gesammelten Daten auf eine CD39-bedingte Wirkung auf die neuronale und astrozytäre Aktivität hin, welche möglicherweise durch Mikroglia vermittelt wird. Ein genereller Mechanismus ist allerdings noch nicht bekannt.
CD39 ist sowohl in einem physiologischen als auch in einem pathophysiologischen Kontext für Mikroglia wichtig. Die hier vorgestellte neuronale und astrozytäre Interaktion in der physiologischen Ebene können somit dazu beitragen, die Pathophysiologie und die Entzündungsprozesse im ZNS besser zu verstehen

3. Introduction

3.1. Purinergic signalling

Purinergic signalling is one of the most important mechanisms for intercellular communication in the nervous system and can be found in all types of cells, alongside its purinergic receptors.

The purine receptors are divided into P1 (metabotropic receptors, activated by adenosine: A_1, A_{2A}, A_{2B} and A_3) and P2 receptors (activated by different nucleotides such as ATP [adenosine 5'-triphosphate] or ADP [adenosine 5'-diphosphate]). P2 receptors are further subdivided into seven ionotropic P2X receptors ($P2X_{1-7}$) and twelve metabotropic P2Y receptors ($P2Y_1$, $P2Y_2$, $P2Y_4$, $P2Y_5$, $P2Y_6$, $P2Y_8$, $P2Y_9$, $P2Y_{10-14}$). P1 and P2 effector responses are usually antagonistic and as such negatively regulate each other, resulting in a tightly regulated system (Fig. 1.1) (Burnstock, 2007; Köles et al., 2011).

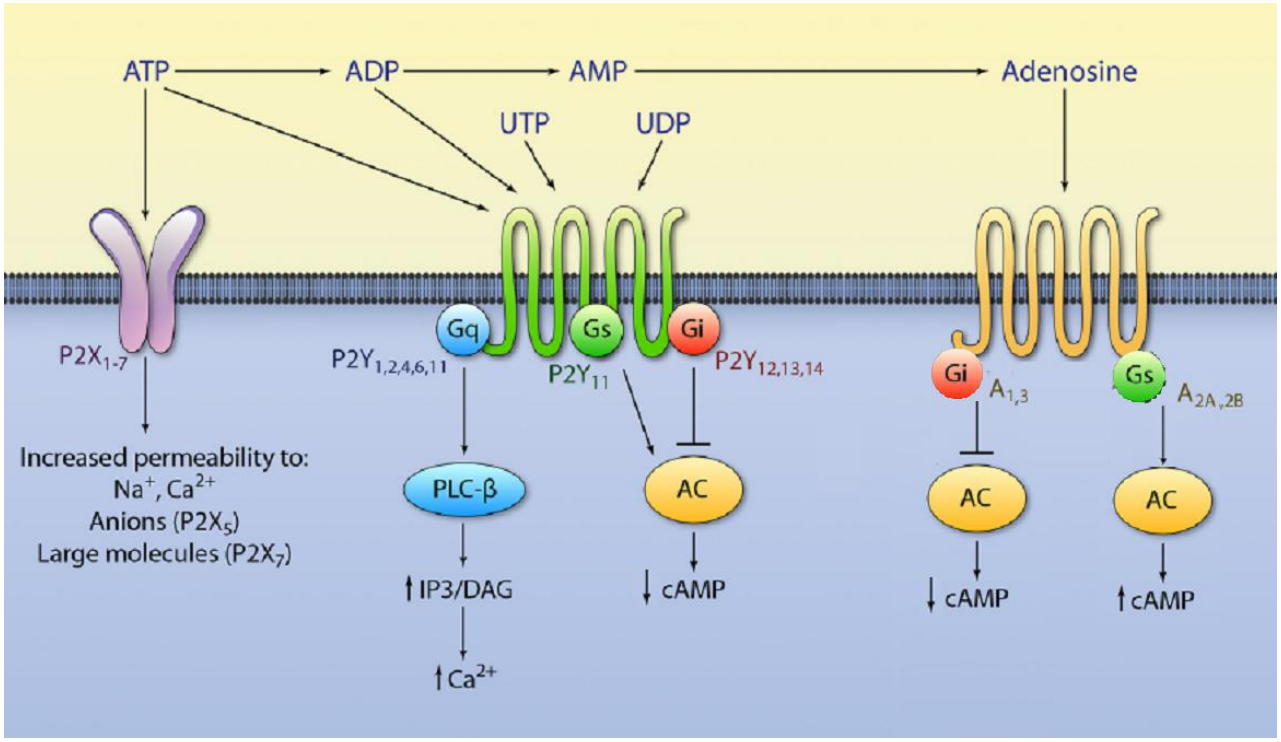

Fig. 1.1 P1 and P2 receptor pathways

P2X channels respond to ATP as their only endogenous ligand and are non-selective cation channels, though some have been demonstrated to allow passage of anions and large molecules.

P2Y receptors are G-protein-coupled receptors. In addition to endogenous ATP and ADP, P2Y receptors respond to the pyrimidines UTP and UDP. $P2Y_1$, $P2Y_2$, $P2Y_4$, and $P2Y_6$ are coupled to G_q to activate phospholipase C (PLC), leading to IP_3-mediated mobilization of intracellular calcium (Ca^{2+}) storage, whereas $P2Y_{12}$, $P2Y_{13}$, and $P2Y_{14}$ couple to G_i and thus inhibit adenylyl cyclase (AC) and cAMP synthesis. $P2Y_{11}$ uniquely couples to both G_q and G_s to increase calcium and cAMP.
P1 receptors are G-protein coupled receptors that bind adenosine and can inhibit (A_1 and A_3 are coupled to G_i) and stimulate AC (A_{2A} and A_{2B} receptors are coupled to G_s), decreasing or increasing cAMP levels, respectively.
Adapted and modified from Yang and Liang, 2012.

ATP is the main purinergic player: it is released from cells by a variety of different mechanisms, such as exocytosis, transporters and diffusion through plasmalemmal channels, as well as being a danger signal released from damaged cells. Once released, various ectonucleotidases sequentially dephosphorylate it to ADP, AMP (adenosine 5'-monophosphate) and adenosine, also signalling molecules in the purinergic pathway. These enzymes can therefore regulate the lifetime of the nucleotides, by de- or rephosphorylation, effectively modulating and terminating P2 receptor functions, as well as activating P1 via degradation of ATP to adenosine (Abbracchio et al., 2009; Verkhratsky et al., 2009).

The ectonucleotidase family is composed by enzymes that metabolize nucleotides on the extracellular space: E-NTPDases (ectonucleoside triphosphate diphosphohydrolases *EC 3.6.1.5*), E-NPPs (ectonucleotide pyrophosphatases / diphosphodiesterases, *EC 3.1.4.1*, *EC 3.6.1.9*), alkaline and acid phosphatases (ALP, *EC 3.1.3.1*, and ACP, *EC 3.1.3.2*, respectively) and ecto-5'-nucleotidase (also known as CD73, *EC 3.1.3.5*) (Fig 1.2). Individual enzymes differ in substrate specificity and product formation. E-NTPDases and E-NPPs hydrolyse ATP and ADP to AMP, which is further hydrolysed to adenosine by ecto-5'-nucleotidase. Alkaline phosphatases equally hydrolyse nucleoside tri-, di- and monophosphates. Dinucleoside polyphosphates, NAD^+ and uracyl 5'-diphosphate (UDP) sugars are substrates solely for E-NPPs. Besides the catabolic pathways, nucleotide interconverting enzymes exist for nucleotide rephosphorylation and extracellular synthesis of ATP (e.g. ectonucleoside diphosphate kinase, *EC 2.7.4.6*, and adenylate kinase, *EC 2.7.4.3*) (Burnstock, 2007; Kukulski et al., 2011).

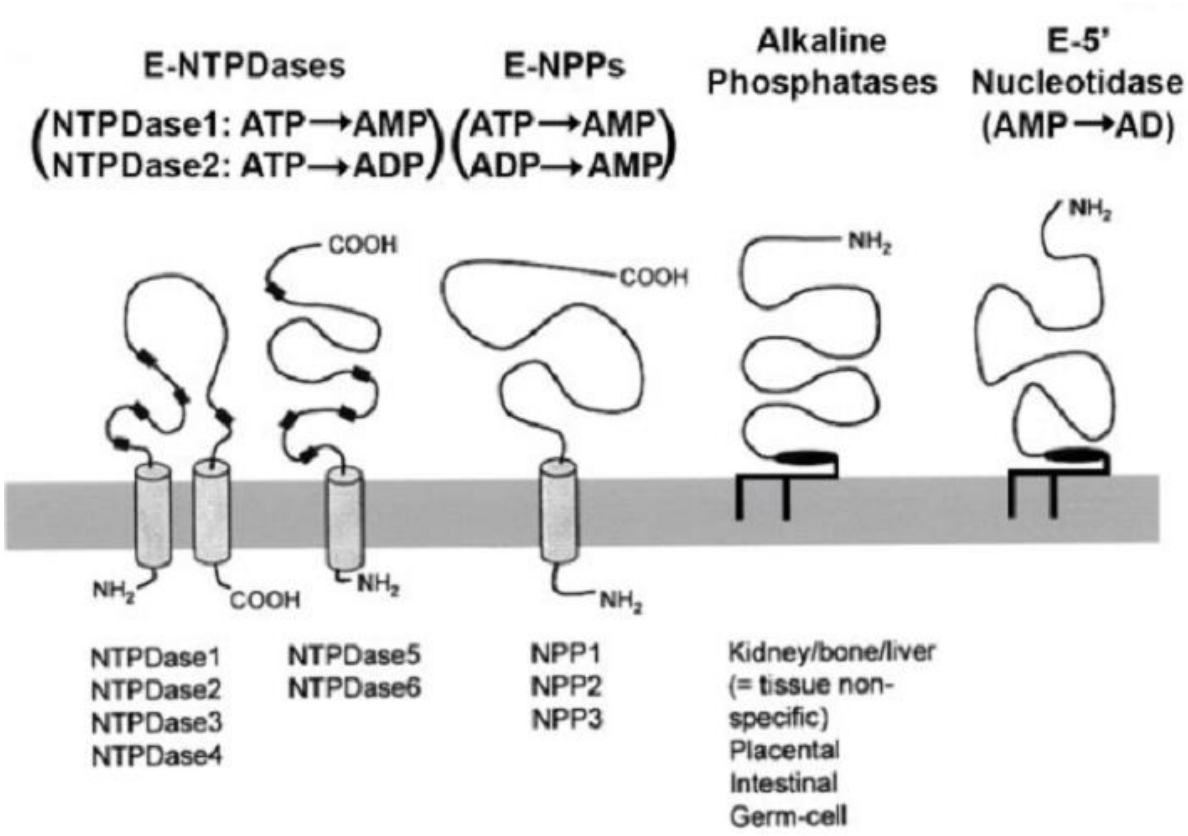

Fig. 1.2 The ectonucleotidase family

Predicted membrane topography of the ectonucleotidases: the E-NTPDase family, the E-NPP family, alkaline phosphatases, and ecto-5'-nucleotidase. From Burnstock, 2007.

3.2. The NTPDase family: regulation of purinergic signalling

The NTPDase family comprises eight members: four located intracellularly – NTPDases 4-7 – and four extracellularly – NTPDases 1, 2, 3 and 8, also referred as E-NTPDases. E-NTPDases 1, 2, 3 and 8 have two plasma membrane spanning domains with an active site facing the extracellular milieu and hydrolyse nucleotides in the range of concentration that activates P2 receptors, making them relevant for the regulation of purinergic signalling (Fig 1.3). All ectonucleotidases are able to hydrolyse tri- and diphosphates with different kinetics and degrees of affinity, solely in the presence of divalent cations calcium (Ca^{2+}) and magnesium (Mg^{2+}) (Kukulski et al., 2005; Robson et al., 2006).

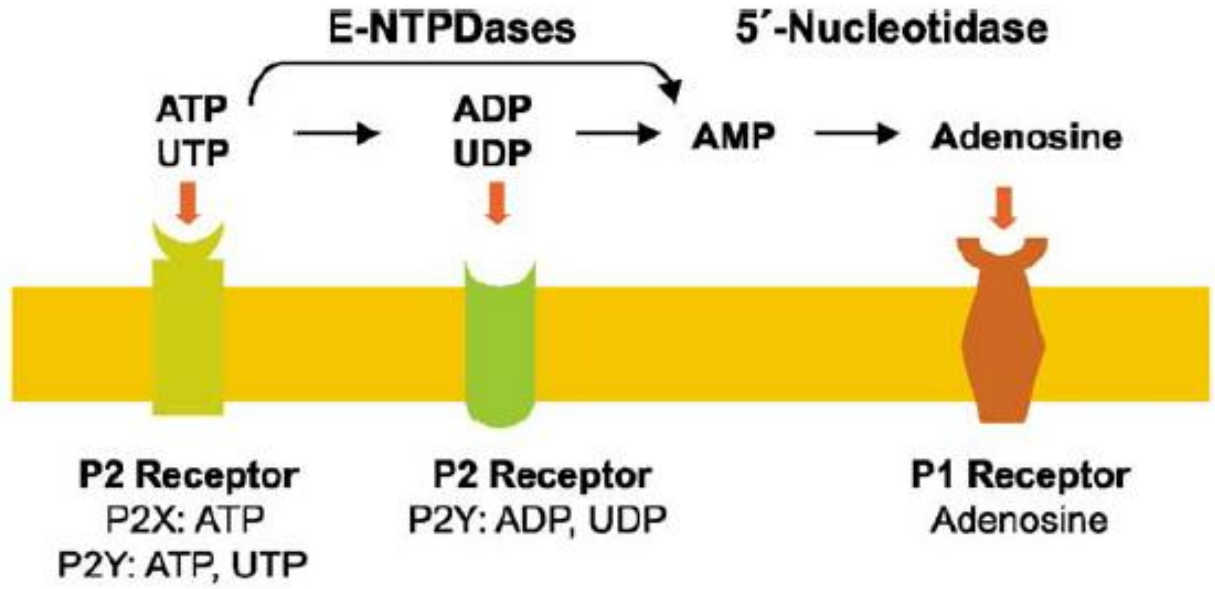

Fig. 1.3 E-NTPDases and ecto-5'-nucleotidases modulate purinergic signalling

Cell surface-located catabolism of extracellular nucleotides and potential activation of P1 and P2 receptors. E-NTPDases sequentially convert ATP to ADP + Pi and ADP to AMP + Pi. E-NTPDase 1 is distinct among these enzymes as it dephosphorylates ATP directly to AMP without the release of significant amounts of ADP. Hydrolysis of the nucleoside monophosphate to the nucleoside is catalyzed by ecto-5'-nucleotidase. ATP can activate both P2X and P2Y receptors whereas UTP activates P2Y receptors subtypes only. After degradation, ADP or UDP may activate additional subtypes of P2Y receptors. The adenosine formed can potentially act on P1 receptors and is either deaminated to inosine or directly recycled via nucleoside transporters. From Robson et al., 2006.

Three ectonucleotidases are expressed in the brain: E-NTPDase 1, 2 and 3 (Braun et al., 2000). Expression in the brain of E-NTPDase 1 (also called CD39) is restricted to microglial cells and vascular endothelium of blood vessels. E-NTPDase 1 rapidly converts both ATP and ADP to AMP, thereby depleting the extracellular space of ligands for P2X and P2Y receptors. E-NTPDase 1 has a Michaelis constant (Km) at least 3 times lower than the other members of this enzyme family, making it an ideal candidate to terminate P2-receptor mediated signalling or prevent the inactivation of purinergic receptors. E-NTPDase 2, expressed by astrocytes, converts preferentially ATP into ADP, but it has a much lower hydrolysis rate for ADP, which can lead to ADP accumulation and subsequent activation of ADP-specific P2 receptors. E-NTPDase 3 is present in hypothalamic neurons. It has substrate preferences intermediate between E-NTPDase 1 and 2, resulting in slower removal of ADP from extracellular space as

compared to E-NTPDase 1, which also results in transient activation of ADP-specific P2 receptors (Kukulski et al., 2005; Robson et al., 2006). While CD39 is present in both microglia and vascular endothelial cells in the brain, they are in opposite sides of the blood-brain barrier (BBB). This physical barrier prevents contact between both cell types, under physiological conditions. Only in exceptional pathophysiological cases, following the disruption of the BBB, would they make contact (Abbott et al., 2010).

3.3. Microglia and purinergic signalling

Microglia are the resident immune cells of the central nervous system (CNS). When faced with a threat to the CNS, microglia change morphology and become motile and amoeboid – *activated* –, and move to a lesion following chemotactic gradients. They are able to clear cell debris, apoptotic cells and microbial pathogens (Kettenmann et al., 2011).

In recent years, various *in vivo* studies have shown that microglia in its normal physiological state still actively scans its surroundings, challenging the notion of “resting” microglia and slowly adopting the classification of “surveying” microglia, which will be adopted throughout this dissertation (Hanisch and Kettenmann, 2007).

Microglia cells express a variety of receptors, including several P2X and P2Y receptors as well as adenosine receptors, which affect multiple cellular responses including microglial activation, proliferation, process motility, migration and release of pro- and anti-inflammatory cytokines (Fig 1.4, Abbracchio et al., 2009).

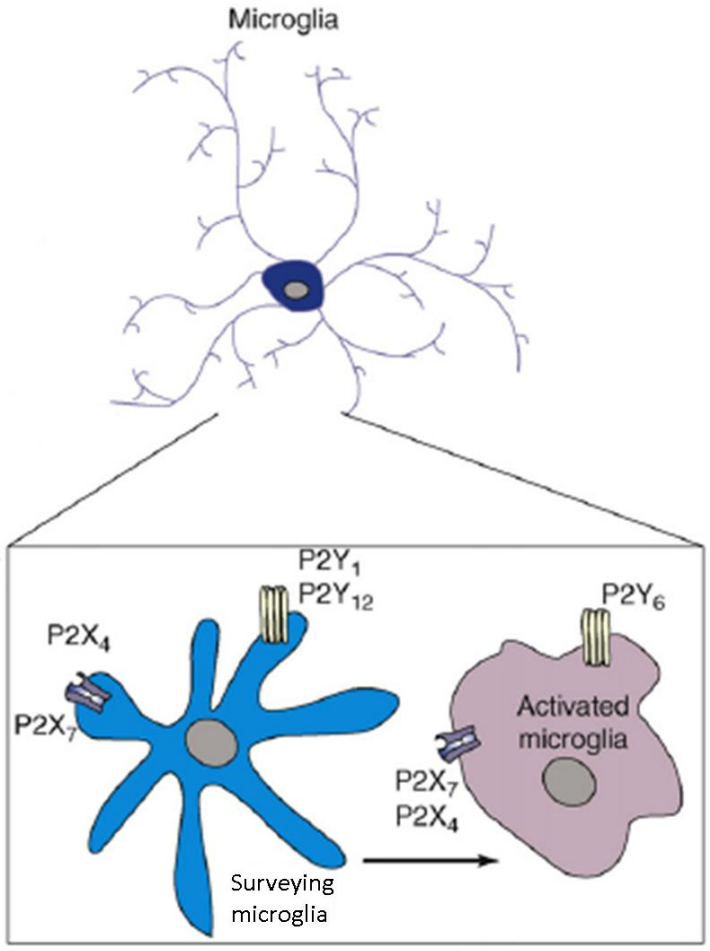

Fig. 1.4 Microglia activation

Purine receptors expressed in microglial cells control their activation process from ramified surveying microglia to amoeboid activated microglia. The purine receptor expression is modified during the process. Modified from Abbracchio et al., 2009.

ATP can be released from damaged or stressed cells (serving as an important danger signal that induces specific immune responses), and from microglia cells themselves (in response to normal physiological responses). This triggers autocrine purinergic feedback mechanisms that are essential regulators of immune cell responses: as mentioned before, microglia have CD39 at their cell membrane, and are able to influence their own amount of purinergic activation (Junger, 2011).

3.4. Neuron-astrocyte interactions: the tripartite synapse

The purinergic signalling system plays a unique role in neuronal–glial interactions, as virtually all types of glia, peripheral (Schwann cells) and central (astrocytes, oligodendrocytes and microglia), express functional purinergic receptors (Abbracchio et al., 2009).
The structural and functional association between neurons and astrocytes is termed the tripartite synapse: it is a synapse composed of the pre- and postsynaptic neuron, associated with the astrocytic process. Neuron-glial interaction, in particular neuron-astrocyte cross-talk, is fundamental for the maintenance of the physiological activity of the brain. Astrocytes sense and integrate synaptic activity and have the ability to release gliotransmitters, among them ATP, glutamate and D-serine (see, for e.g., Halassa et al., 2007).

In neurons, ATP can be co-stored in secretory and synaptic vesicles and co-released with other neurotransmitters into the extracellular space (some neuronal terminals [e.g. in the *medial habenula* and in the cortex] might contain pools of ATP-only vesicles) (Abbracchio et al., 2009). After release, ATP undergoes rapid enzymatic degradation to ADP and AMP, which is further hydrolysed to adenosine. Besides the catabolic pathways, nucleotide-interconverting enzymes exist for nucleotide rephosphorylation and extracellular synthesis of ATP. Extracellular adenosine originates either from the catabolism of nucleotides by ectonucleotidases or by cellular reuptake through equilibrative nucleoside transporters (ENTs) or concentrative nucleoside transporters (CNTs) (Halassa et al., 2007; Halassa et al., 2009).

Astrocytes respond to neurotransmitter release with elevation of their Ca^{2+} levels. In culture and *in vivo*, elevation of the Ca^{2+} signal within one astrocyte can lead to a calcium wave that propagates through the coupled glial network (Fig. 1.5 a). Calcium wave propagation is described by two mechanisms: (1) ATP is released from astrocytes onto the extracellular space and activates purinergic receptors in neighbouring astrocytes, leading to elevation of internal Ca^{2+}; and (2) diffusion of inositol 1,4,5-trisphosphate [$Ins(1,4,5)P_3$] through gap junctions, binding to its receptor and causing the release of Ca^{2+} from internal stores (Fig. 1.5 b) (Halassa and Haydon, 2010).

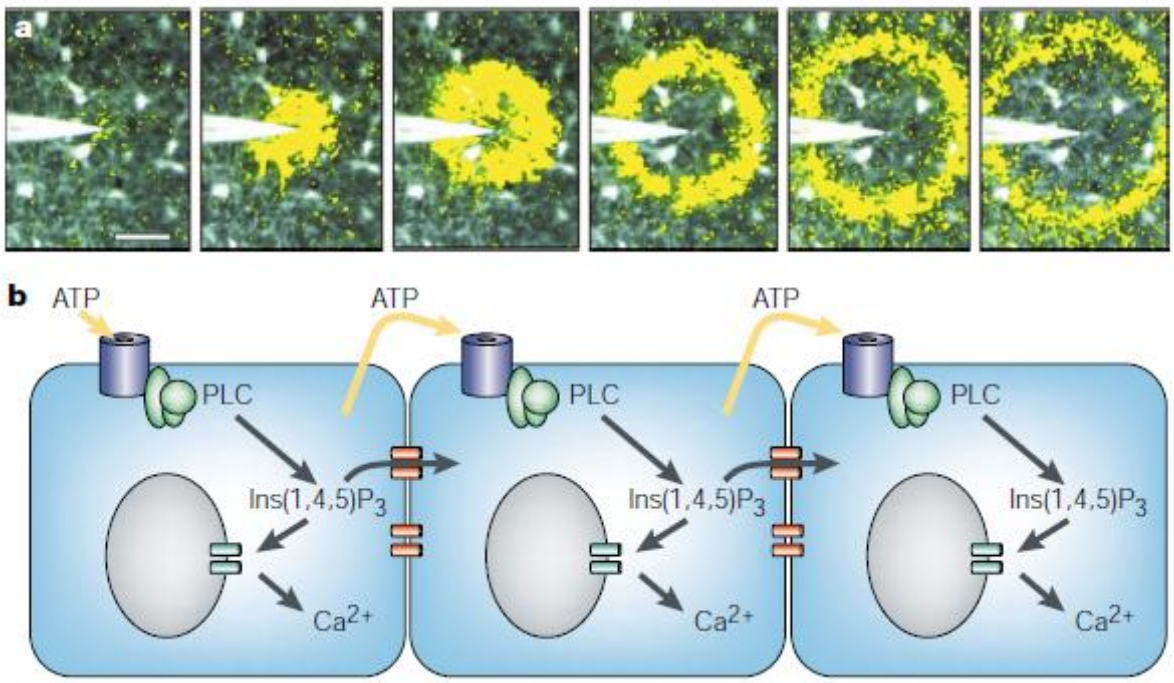

Fig. 1.5 Glial calcium waves

a) Stimulation of glial cells from the retina evokes a radially propagating Ca^{2+} wave

Mechanical stimulation of a glial cell in the centre of the field of view evoked a local elevation of Ca^{2+} that propagated to neighbouring cells.

b) Mechanism for glial calcium wave generation

Ca^{2+} is released from internal stores in response to elevated internal inositol 1,4,5-trisphosphate [Ins(1,4,5)P_3]. Neurotransmitters can engage astrocytic metabotropic receptors, a subset of which couples through G_q proteins to phospholipase C (PLC), resulting in the accumulation of diacylglycerol (DAG) and Ins(1,4,5)P_3. Ins(1,4,5)P_3 can diffuse to neighbouring cells through gap junctions to cause short-range signalling. Longer-range calcium signalling requires the release of ATP, which causes the regenerative production of Ins(1,4,5)P_3 and further release of ATP from neighbouring astrocytes.

From Haydon, 2001.

Regulated release of ATP from glial cells plays an important role in both glial–glial signalling (e.g. astrocytic calcium waves) and in glial–neuronal communications (e.g. modulating neuronal responses). Other gliotransmitters are instrumental in shaping neuronal responses, such as astrocytical glutamate modulates NMDA-neuronal responses. Finally, release of ATP is responsible for proliferation, process motility and migration of microglia, thus reflecting its role in the health maintenance of the CNS (Fig. 1.6) (Halassa and Haydon, 2010; Verkhratsky et al., 2009).

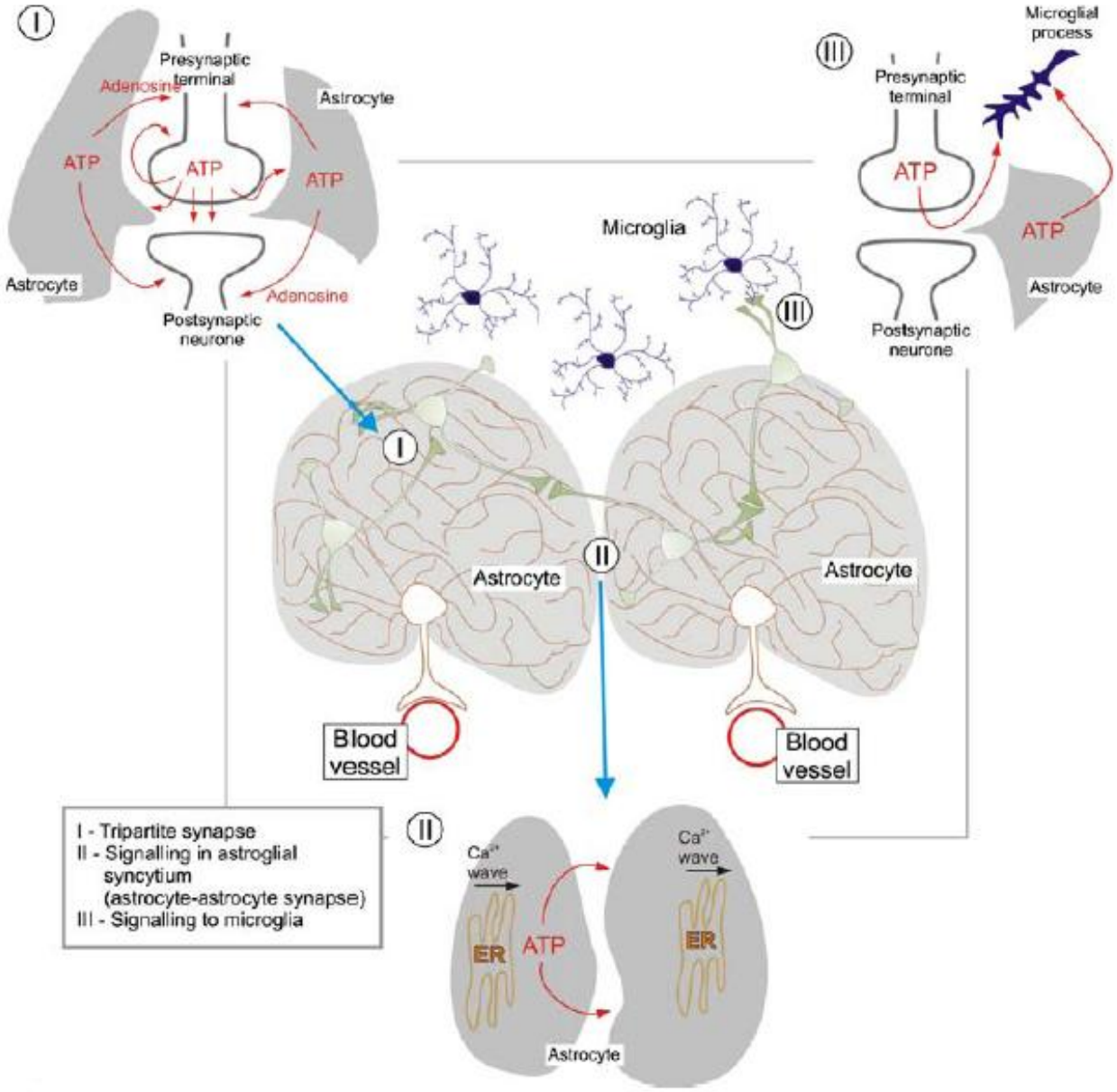

Fig. 1.6 Purinergic signalling pathways in neuronal–glial circuits in the grey matter

The microarchitecture of the grey matter (as shown in the centre) is defined by astroglial domains, composed of astrocyte, neighbouring blood vessel encompassed by astroglial endfeet and neurons residing within astroglial territory. The microglial cells (each also having its own territory) are constantly surveying these domains for damage. ATP and its derivatives act as an extracellular signalling molecule at all levels of communications within neuronal–glial networks. Within the tripartite synapse (I), ATP, released during synaptic transmission, activates astrocytical receptors, which in turn initiate Ca^{2+} signals and Ca^{2+} waves in the astroglial syncytium. Astroglial Ca^{2+} signals induce release of ATP, which feeds back to neurons via activation of pre- and postsynaptic P1 and P2 receptors. ATP released from astrocytes (II) triggers and maintains astroglial Ca^{2+} waves. Finally, ATP released from all types of neural cells control activation (III) of microglia. Modified from Verkhratsky et al., 2009.

3.4.1. The barrel cortex as a study model for neuron-astrocyte interactions

The barrel cortex is part of the somatosensory cortex in the brain of most rodents. It receives and processes tactile information derived from the whiskers on the contralateral face of the animal. The neuronal pathway connecting the whiskers to the barrel cortex travels through the brain-stem, thalamus, and then terminates primarily in the cortex (Agmon and Connors, 1991). In cross-section, the cortex is a six-layered structure where the main input layer is layer IV and where the barrels that give the barrel cortex its name are located. The barrels identify the location of vertical cortical columns, a fundamental element of cortical structure which represents its sensory units: each column responds to the movement of a single whisker of the animal (Fox, 2002). Indeed, *in vivo* stimulation of an individual mouse whisker induces Ca^{2+} signals in astrocytes located in the corresponding cortical barrel (Wang et al., 2006). The well-known anatomofunctional organization of neurons in the barrel cortex offers an ideal model to study neuron-astrocyte interactions: e.g., astrocytes respond to activation of layer IV but not layers II/III, consistent with a systematic position on the overall flow of activity (Fox, 2002).

Previous studies from our lab illustrate the astrocytes' ability to respond (via Ca^{2+} increase) to layer IV neuronal activity, and such a response was restricted to the same sensory column (Schipke et al., 2008). Additionally, it was found that astrocytes control neuronal activity via a GABA-mediated mechanism (Benedetti et al., 2011).

3.5. Aim of the project

The aim of the present study was to assess the effect of CD39 on neuronal and astrocytical functions. Previous studies have focused on the blood haemostasis disorders associated with endothelial cells lining the vasculature (Enjyoji et al., 1999) or with microglia-specific functions, such as migration (Färber et al., 2008) or phagocytosis

(Bulavina et al., 2013). To our knowledge, this is the first work describing neuron-glia effects modulated by CD39.

Considering the pivotal role of purinergic signalling in the CNS, it is important to determine how CD39 from microglia can influence astrocytes. Accordingly, we aim to understand this glia-glia mechanism. Another component entails understanding the extent of glia-neuronal signalling in these conditions and possibly describe a mechanism of action.

This study can help understand the physiological relevance of CD39, which will give insights into its role in pathophysiology and ultimately understand how inflammation modulates neuronal and astrocytic activity in the CNS.

4. Materials

4.1. Chemicals

Chemical	Company
ADP (Adenosine 5'-diphosphate)	Sigma-Aldrich, Munich, Germany
ATP (Adenosine 5'-triphosphate)	Sigma-Aldrich, Munich, Germany
Apyrase	Sigma-Aldrich, Munich, Germany
ARL 67156 (6-*N*,*N*-Diethyl-D-β,γ-dibromomethyleneATP trisodium salt)	R&D Systems GmbH, Wiesbaden-Nordenstadt, Germany
dNTP	Invitek, Berlin, Germany
Ethidium bromide	Carl Roth, Karlsruhe, Germany
Fluo-4 acetoxymethyl (AM) ester	Invitrogen, New York, USA
Hank's balanced salt solution (HBSS)	GIBCO®, Invitrogen, Darmstadt, Germany
HEPES	Carl Roth, Karlsruhe, Germany
PPADS (Pyridoxalphosphate-6-azophenyl-2',4'-disulfonic acid tetrasodium salt)	Tocris Bioscience, Bristol, UK
Sulphorhodamine 101	Sigma-Aldrich, Munich, Germany
TaKaRa Ex Taq Hot Start polymerase	TaKaRa, Madison, USA
Trichloroacetic acid (TCA)	Sigma-Aldrich, Munich, Germany

Table 1. List of chemicals

4.2. Buffers and solutions

Buffer / Solution	Content
Artificial Cerebro-Spinal Fluid (ACSF)	134 mM NaCl, 2.5 mM KCl, 1.3 mM $MgCl_2$, 2 mM $CaCl_2$, 1.26 mM K_2HPO_4, 10 mM D-Glucose, 26 (RT, for storing prior to experiment) or 21,4 mM (34ºC, recording chamber) $NaHCO_3$; pH 7.4
Dulbecco's Modified Eagle Medium (DMEM)	Supplemented with 10% heat inactivated fetal calf serum, 2 mM L-glutamine,100 U mL^{-1} penicillin, 100 µg/mL streptomycin
L929 conditioned medium.	L929 mouse fibroblast cells at 80% confluency were overlaid with 30 mL supplemented DMEM.

	After 2 days conditioned medium was collected, filtered and frozen until usage
PBS	137 mM NaCl, 2.7 mM KCl, 4.3 mM Na_2HPO_4, 1.4 mM KH_2PO_4; pH 7.4
Phosphate-free reaction buffer for Malachite Green Assay	20 mM HEPES, 135 mM NaCl, 5 mM KCl, 1.8 mM $CaCl_2$, 1 mM $MgCl_2$, 5.6 mM D-Glucose
Pipette internal solution	120 mM K-Gluconate, 10 mM KCl, 1 mM $MgCl_2$, 0.1 mM EGTA, 0.025 mM $CaCl_2$, 10 mM HEPES, 1 mM $ATPK_2$, 0.2 mM GTPNa, 4 mM D-Glucose
Trypsin/DNase mix	10 mg Trypsin, 0.5 mg DNase per mL of PBS

Table 2. List of buffers and solutions

4.3. Primers

Specificity	**Sequence**
CD39 $^{+/+}$, forward (D3M)	5'ACT GTT TAT ATC CCA AGG AGC TGG CAT AGG 3'
CD39 $^{+/+}$, reverse (MEC8P)	5'GAC AGA CGA GGG AAG AGG AAG G 3'
CD39 $^{-/-}$, forward (D3M)	5'ACT GTT TAT ATC CCA AGG AGC TGG CAT AGG 3'
CD39 $^{-/-}$, reverse (NEOP2)	5'TAC CCG TGA TAT TGC TGA AGA GCT TGG CGG 3'

Table 3. Primers to genotype CD39 mice

4.4. Kits

Description	**Company**
BCA total protein assay	Pierce Biotechnology, Rockford, USA
Malachite Green Phosphate Assay Kit	BioAssay Systems, Hayward, USA
peqLAB DirectLyse Tail Kit	peqlab, Erlangen, Germany

Table 4. List of kits

4.5. Equipment and Devices

Description	Company
CCD Camera (Sensicam QE)	PCO AG, Kelheim, Germany
Centrifuge Eppendorf 5417R	Eppendorf, Hamburg, Germany
EPC 9 Patch Clamp Amplifier	HEKA Elektronik Dr. Schulze GmbH, Lambrecht/Pfalz, Germany
Eppendorf Thermomixer 5355	Eppendorf, Hamburg, Germany
G24 Shaker incubator	New Brunswick Scientific, Edison, USA
Microplate plate reader Infinite M200	Tecan, Crailsheim, Germany
Monochromator	Till Photonics, München, Germany
Neurolog Stimulator	Digitimer, Hertfordshire, UK
T3000 thermocycler	Biometra, Göttingen, Germany
Upright fluorescence microscope	Zeiss, Oberkochen, Germany
Vibratome HM650V	Microm International GmbH, Walldorf, Germany

Table 5. List of equipment and devices

4.6. Computer software

Software	Company
Adobe Acrobat 9 Professional	Adobe Systems, USA
Adobe Illustrator CS5	Adobe Systems, USA
Camware	PCO AG, Kelheim, Germany
Image J 1.47	http://rsbweb.nih.gov/ij/index.html
Mendeley Desktop	Mendeley Ltd
Microsoft Office 2010	Microsoft Deutschland, Berlin, Germany
Origin	Origin Lab, USA
Peak Count 3.2.1	Christian Henneberger, Berlin, Germany
TIDA	HEKA Elektronik, Lambrecht, Germany

Table 6. List of computer software

5. Methods

5.1. Animals

Animals were kept for breeding in the MDC animal facility under approved housing conditions (TVV 0014/08, according to Landesamt für Gesundheit und Soziales Berlin [LAGeSo]). All animals were handled according to governmental and internal (MDC) rules and regulations. CD39 $^{+/+}$ and CD39 $^{-/-}$ mice were kept in a 12h light / dark cycle and received food and water *ad libitum*.
Due to restrictions in breeding, both male and female mice were used for experiments.

5.2. Genotyping of CD39 $^{+/+}$ and CD39 $^{-/-}$ mice

DNA for genotyping was isolated from tailcuts using the peqLABDirectLyse Tail Kit according to manufacturer's instructions. Briefly, 100 µL Direct Lyse together with 10 µL Proteinase K was added to the tail tip and incubated for 3h at 55°C. The lysis was stopped with 45 min of incubation at 85°C. After the centrifugation at 16000g for 10 min, the supernatant was kept at -20°C until used for PCR.

CD39 $^{-/-}$ mouse:

Tail DNA	5,0 µL
Primer forward **D3M** (25 µM)	0,5 µL
Primer reverse **NEOP2** (25 µM)	0,5 µL
dNTP (10mM)	0,5 µL
10x reaction buffer	2,5 µL
TaKaRa Ex Taq polymerase	0,25 µL
ddH2O	15,75 µL

Table 7. PCR composition to genotype CD39 $^{-/-}$ mice

CD39 $^{+/+}$ mouse:

Tail DNA	5,0 µL
Primer forward **D3M** (25 µM)	0,5 µL
Primer reverse **MEC8P** (25 µM)	0,5 µL
dNTP (10mM)	0,5 µL
10x reaction buffer	2,5 µL
TaKaRa Ex Taq polymerase	0,25 µL
ddH2O	15,75 µL

Table 8. PCR composition to genotype CD39 $^{+/+}$ mice

PCR amplification parameters were set as follows:

Reaction	Temperature, °C	Time
Initial Denaturation	94	1 min
30-33 Cycles:		
Denaturation	94	15 sec
Annealing/ Elongation	66	3 min 30 sec
Final polymerization	72	10 min

Table 9. PCR program to genotype CD39 mice

The products of the PCR were then loaded on the 1.5 % agarose gel with 0.5 µg/mL ethidium bromide and were subjected to electrophoresis in TAE running buffer. The separated fragments were analysed under UV light (254 nm).

5.3. Microglia cell cultures

5.3.1. Microglia cell culture preparation

Microglia cultures were prepared from cerebral cortex of newborn CD39 $^{+/+}$ and CD39 $^{-/-}$ mice. The whole isolation procedure was performed on ice. Brains from newborn mice were collected in Hank's Balanced Salt solution (HBSS). Forebrains were carefully freed of blood vessels and meninges. After washing three times with HBSS, cortical tissue was incubated for 2 min with a Trypsin/DNase mix. The reaction was stopped by

addition of Dulbecco's modified Eagle's medium (DMEM) supplemented with 10 % fetal calf serum (FCS), 2 mM L-glutamine, 100 U mL^{-1} penicillin, and 100 µg/mL streptomycin. Finally, cell mixture was incubated with DNase, dissociated with a fire-polished pipette and washed twice. Mixed glial cells were cultured in complete DMEM in T75 flasks until confluency. Cultures need to be washed carefully every third day to remove cell debris by several replacements of the medium with PBS and strong shaking. After establishment of an astrocytic monolayer, checked by morphology under a microscope, the medium was changed to DMEM (10% FCS, supplemented with L-glutamine, penicillin and streptomycin) containing 30% L929 conditioned medium and incubated for 3 days. Microglial cells were then separated from the underlying astrocytic layer by gentle shaking of the flasks for 1h at 37°C in a shaker incubator (100 rpm). The cells were seeded in 96-well plates at a density of 2 x 10^4 or 10^5 cells / well, respectively. Cultures usually contained 95 % microglial cells, which can be checked by staining with tomato lectin, a marker for microglia. Cultures were used for experiments 1 to 3 days after plating.

5.3.2. Measurement of extracellular ATP degradation in microglial cultures using Malachite Green phosphate assay

The concentration of free phosphate in the reaction buffer of microglial cultures was measured with the Malachite Green phosphate assay (BioAssay Systems, Hayward, USA). The assay is based on the quantification of the green complex formed between Malachite Green, molybdate and free phosphate. The colour formation was measured on a plate reader (Tecan, Crailsheim, Germany).

Free phosphate is released to the reaction buffer by the cells themselves (basal level), but mostly due to the enzymatic cleavage of the extracellular purines. Therefore, the activity of CD39 on microglia cultures was evaluated by adding 1 mM ATP, 1 mM ADP or free-phosphate reaction buffer (100 µL per well, 96-well plates) to the cells. In parallel, the solutions of ATP, ADP and phosphate-free reaction buffer were placed into the plate without any cells as a positive control for the spontaneous degradation of purines or any free phosphate contamination in the solutions. After 10 min of incubation at 37°C, the reaction was stopped by adding 20 µL of 10% TCA to 90 µL of cell

supernatant and the plate was placed on ice. Next, the samples were diluted 1:5 with phosphate-free reaction buffer, to avoid the development of a very intense signal or precipitation.

Phosphate standards were prepared for calibration: 80 µL of test samples and standards were transferred into the separate wells of the 96-well plate. Working Reagent was prepared by mixing the Reagent A and Reagent B at a 1:100 ratio. 20 µL of Working Reagent per well was added to the samples and standards and the chromogenic reaction was developed after 30 min at room temperature (RT). Optical density (OD) was measured on the plate reader at 620 nm. OD_{620nm} was then plotted versus standard phosphate concentrations. Sample phosphate concentrations in µM were determined from standard curve. All tests were performed in triplicate.

For the final expression of enzymatic activity, free phosphate concentrations were normalized to the corresponding amount of protein (see below, *3.3.3 Protein measurement in microglial cultures using the BCA kit*). Enzymatic activity was then presented as: [Phosphate], µM / mg protein / minute.

5.3.3. Protein measurement in microglial cultures using the BCA Kit

The BCA assay (Pierce Biotechnology, Rockford, USA) is based on the reduction of Cu^{2+} to Cu^{1+} by protein in an alkaline medium with the colourimetric detection of the cuprous cation (Cu^{1+}) by bicinchoninic acid (BCA). The intense purple-coloured reaction product results from the chelation of two molecules of BCA with one cuprous ion.

For microglia cell cultures, cells were lysed with 0,02% w/v SDS (50 µL per well in 96-well plates) for 20 min at RT, with agitation. Afterwards, 25 µL of each standard and unknown sample were placed into the separate wells of microplate and 200 µL of Working Reagent (a mix of 50:1 Reagent A with Reagent B) was added per well. The reaction was developed over 30 min in a wet chamber at 37°C. The plate was cooled to RT and the absorbance was measured at 562 nm on a Tecan plate reader. OD_{562nm} was then plotted versus standard BSA concentrations. Sample protein concentrations in mg / mL were determined from standard curve.

5.4. Acute brain slices

5.4.1. Preparation of acute brain slices

Acute brain slices were prepared from young mice (P8-P10). Depending on the experimental design, thalamocortical (Agmon and Connors, 1991) or coronal slices (Schipke et al., 2002) were prepared.
After decapitation, brains were quickly isolated and washed in ice-cold artificial cerebrospinal fluid (ACSF).

For thalamocortical slices, the cerebellum was removed and the forebrain was cut off in an angle of about 55º to the right of the posterior-to-anterior axis of the brain, and placed onto that plane in the metal stage. For coronal slices, the cerebellum was removed; the brain was placed upright (with olfactory bulbs upward) onto the metal stage. In both cases, 250 µm slices were cut in ice-cold ACSF with a vibratome (HM 650 V, Microm International GmbH, Walldorf, Germany).
Slices were then carefully transferred onto the nylon grid in the ACSF at RT, continuously saturated with carbogen (95% CO_2, 5% O_2). Acute brain slices can be kept in ACSF, saturated with carbogen, for up to 6h.

5.4.2. Calcium imaging in acute brain slices: induction of calcium waves in the corpus callosum

After acute slice preparation from young mice (see *Preparation of acute brain slices*), coronal slices were incubated with the calcium indicator dye Fluo-4-acetoxymethylester (10 µM Fluo-4 AM, Invitrogen, New York, USA) for 45 min at RT with constant perfusion with carbogen.
Slices were then transferred to a perfusion chamber on an upright microscope (Zeiss, Oberkochen, Germany) and fixed in the chamber by using a U-shaped platinum wire with a grid of nylon threads. The perfusion was continuously gassed with carbogen and had a constant flow of 5 mL min^{-1}. All experiments were performed with bath solution and drugs at 32-34ºC. Drugs were applied by changing the perfusate. Intracellular

calcium changes were detected by a CCD camera (PCO AG, Kelheim, Germany), with a sampling rate of 1 Hz. A monochromator set to 488 nm (Till Photonics, München, Germany) was used as a light source for fluorophore excitation.
Electrical stimulation was accomplished with a conventional glass electrode filled with bath solution. The pipettes had a resistance of ≈ 1 MΩ, which corresponds to a tip opening of ≈ 15 µm. The tip of the pipette was placed on the *corpus callosum*, at the top of the slice, with the pipette only gently touching the upper cell layer. After the positioning of the pipette the slice was allowed to recover from mechanical stress for at least 2 min.
The wave was elicited by applying 10 Hz stimulation for 4s, 30 µA. This stimulation paradigm was chosen as it induced solid responses. The calcium wave could be triggered repetitively within the same area, allowing the time between stimulations to be at least 5 min (Schipke et al., 2002).

5.4.3. Electrophysiology in acute brain slices: patch-clamping of neurons in the barrel cortex

After acute slice preparation from young mice (see *Preparation of acute brain slices*), thalamocortical slices rested for 45 min with ACSF at RT with constant perfusion with carbogen.
Slices were then transferred to a perfusion chamber on an upright microscope (Zeiss, Oberkochen, Germany) and fixed in the chamber by using a U-shaped platinum wire with a grid of nylon threads. The perfusion was continuously gassed with carbogen and had a constant flow of 5 mL min^{-1}. All experiments were performed with bath solution and drugs at 32-34ºC. Drugs were applied by changing the perfusate. Intracellular calcium changes were detected by a CCD camera (PCO AG, Kelheim, Germany), with a sampling rate of 1 Hz.

Barrel fields were identified in bright field illumination. Neurons were patched under bright-field illumination using a 40x objective. The sample of neurons chosen is a heterogeneous group of excitatory neurons composed of pyramidal cells and spiny stellate cells. The shape of cell somata was used as criteria of neuron selection:

triangular for pyramidal cells (layer II/III) and small and round for spiny stellate cells (layer IV). Sulforhodamine 101 (Sigma-Aldrich, Munich, Germany) was added in concentration of 0.1 mg mL^{-1} to the pipette solution for neuron morphological identification (Benedetti et al., 2011).

Whole-cell recordings were obtained in current clamp mode and action potentials were elicited by injecting current steps. Local barrel stimulation was applied through a glass electrode (tip opening ≈ 20 µm) placed in layer IV of the cortex within a given barrel field. The stimulus consisted of 30 voltage pulses at 4 V, 30 µA, duration of a single stimulus 1 ms (Schipke et al., 2008). For stimulation, the amplifier voltage output was connected to an external stimulus isolator (NeuroLog NL 800, Digitimer Ltd, Welwyn Garden City, UK).

Voltage signals were amplified (EPC 9, HEKA Elektronik, Lambrecht, Germany), sampled (10 kHz), and monitored with TIDA software (HEKA Elektronik, Lambrecht, Germany).

5.5. Statistical analysis

For patch-clamp data analysis and statistics, TIDA (HEKA Elektronik, Lambrecht, Germany), Origin (Origin Lab, USA) and Microsoft Excel were used. The analysis of the synaptic currents was performed with Peak-Count software (Version 3.2.1) developed by Christian Henneberger at the Physiology Department of the Charité (Berlin, Germany), using a first-derivative threshold detection algorithm.

The stimulus-evoked depolarization in neurons was measured at time points when no action potential occurred. The integral of stimulus-evoked depolarization over time (I STM) was determined from the baseline at the resting voltage and included also the time course of action potentials.

Fluo-4 fluorescence recordings were normalized ($F/F0$) and filtered using a median filter with Image J. $F0$ was obtained by averaging 10 frames at the beginning of the recording. To determine the area occupied by the calcium wave, images prior to, between and 1–3 s after stimulation were compared. The area was composed of pixels

which increased in brightness above threshold. Lateral drift of the imaged field induced by movements of the sample during the experiment was manually corrected.

Since the calcium wave is being evoked in a brain slice, the tissue is heterogeneous (particularly in the *corpus callosum*, where the wave follows the direction of the axonal tracts) and as such does not always spread in a circular fashion, like in astrocyte cultures (Fig. 1.4 a) , but more elliptical and irregular (see Fig. 3.1) As such, the analysis of the calcium waves could not be measured in distance over time (as is usual for the study of calcium waves in homogenous populations of astrocytes in culture). The standard chosen was the total area of the spread of the calcium wave: the frames showing the wave propagation selected, averaged into a single frame and the total area measured.

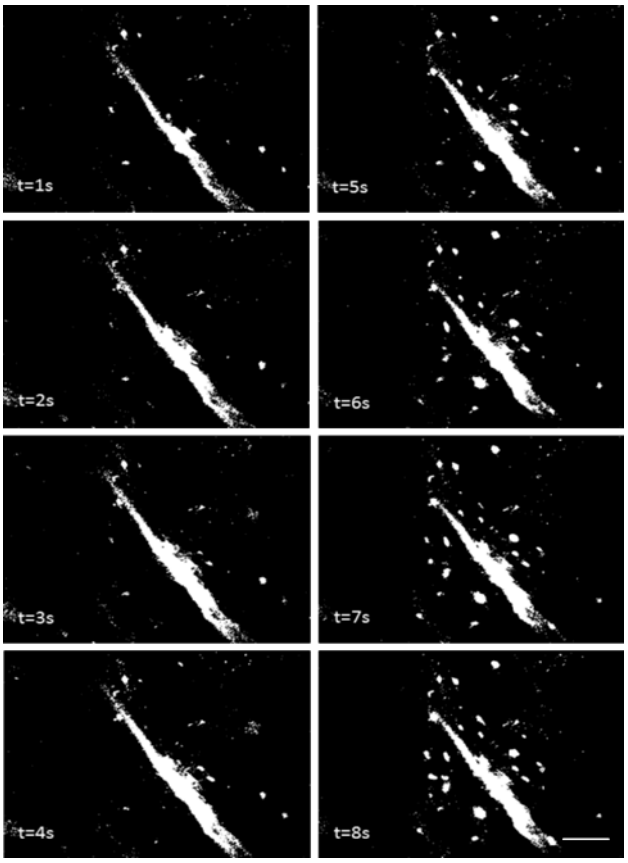

Fig. 3.1 Binary images of a calcium wave spreading over time
Scale bar 100µm.

Statistical significance was determined by the parametric T-Test according to the distribution and is depicted as *: $p < 0.05$, **: $p < 0.01$, ***: $p < 0.001$. Data are presented as mean ± s.e.m.

6. Results

6.1. Nucleotides are metabolized by CD39 present in microglia

To analyse the enzymatic activity of CD39, the phosphate assay with the Malachite Green assay was performed in microglia cell cultures.
Cell cultures were incubated with 1 mM ATP, 1 mM ADP or free-phosphate reaction buffer and free phosphate was measured in the supernatant using the Malachite Green assay. In parallel, the solutions of ATP, ADP and phosphate-free reaction buffer were placed into the plate without any cells as a control for the spontaneous degradation of purines or any free phosphate contamination in the solutions. The levels of phosphate measured in these controls were subtracted from the experimental values.

6.1.1. Microglia in CD39 $^{-/-}$ mice do not metabolize ATP or ADP (in vitro)

In microglia cell culture, CD39 $^{+/+}$ cells metabolized both extracellular ATP and ADP (9.59 ± 1.00 and 4.97 ± 0.51 µmol phosphate / mg protein / min, respectively), with 1.9-fold more enzymatic activity for ATP than ADP (n = 9). In CD39 $^{-/-}$ cells, there was no ATP- nor ADP-dephosphorylation activity detected (n=11, Fig. 4.1).

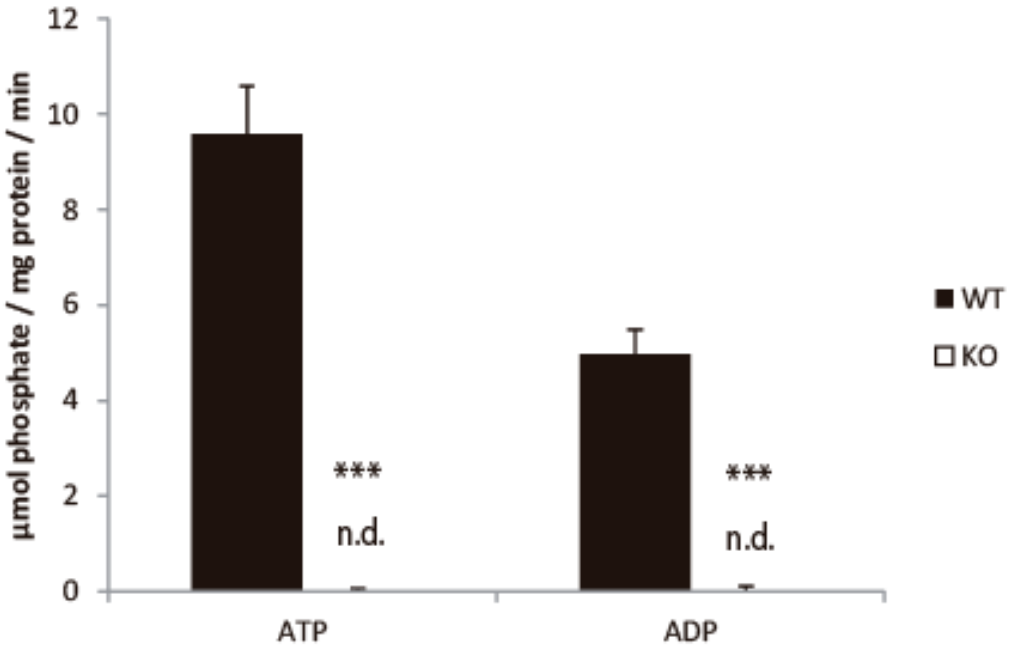

Fig. 4.1 Nucleotides are metabolized by CD39 in microglia culture

In microglia cell culture, ATP and ADP are not metabolized by CD39 $^{-/-}$ cells.

*** for $P < 0.001$, t-test.

6.2. Astrocyte-mediated calcium waves are influenced by microglial CD39

Calcium waves are evoked by astrocytes and propagate via gap junctions and/or an ATP regenerative mechanism (Fig. 1.4 b). Previous experiments show that while this is true for the grey matter, in the white matter the calcium wave propagation is restricted to the ATP mechanism. Furthermore, it is independent from neuronal activity (Schipke et al., 2002). This makes the white matter, specifically the *corpus callosum*, an ideal area to study glia interactions.

To investigate if CD39 – present in microglia – has an effect on astrocyte-evoked calcium waves, experiments in acute brain slices were designed.

6.2.1. Calcium waves spread further in CD39 $^{-/-}$ mice

Calcium waves were evoked electrically (see Methods) in acute brain slices, on the *corpus callosum* in wild-type and knock-out mice.

In slices from CD39 $^{-/-}$ mice, the calcium wave area was 16667.82 ± 2489.21 µm^2 (n = 32), 2.8-fold higher than in CD39 $^{+/+}$, 5900.88 ± 690.26 µm^2 (n = 32, P = 4 x 10^{-6}, Fig. 4.2).

Fig. 4.2

A

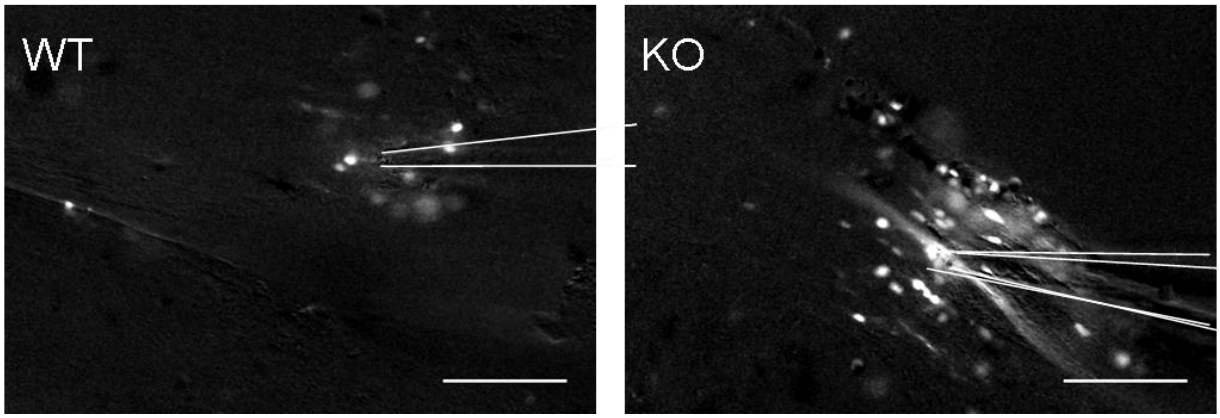

B **Calcium waves spread more in KO than in WT mice**

(A)

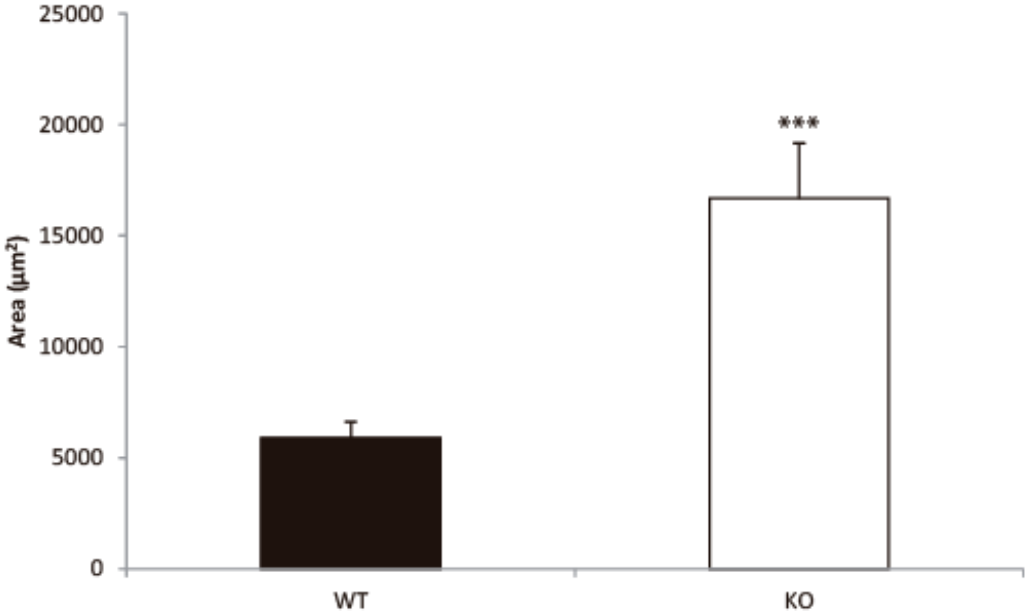

Calcium wave in acute brain slices from wild-type (WT) and knock-out (KO) mice. White lines represent stimulation pipette. Scale bar 100 µm.

(B) Calcium waves are electrically evoked on wild-type and knock-out mice, the wave spreads significantly more in the knock-out.

*** for P < 0.001, t-test

6.2.2. Calcium waves are purine-dependent

To assess dependency of calcium waves from the purinergic pathway, PPADS (a broad purinergic receptor blocker) was applied to acute brain slices of CD39 $^{+/+}$ and CD39 $^{-/-}$ mice.

In CD39 $^{+/+}$, PPADS application (100 µm) decreased significantly the area of calcium wave from 9546.63 ± 1139.36 µm^2 to 2466.51 ± 759.07 µm^2 (n = 9, P = 5 x 10^{-5}). In CD39 $^{-/-}$, the decrease was more accentuated: from 17997.93 ± 3864.06 µm^2 to 5056.91 ± 318.77 µm^2 with PPADS application (n = 8, P = 0.04, Fig. 4.3).

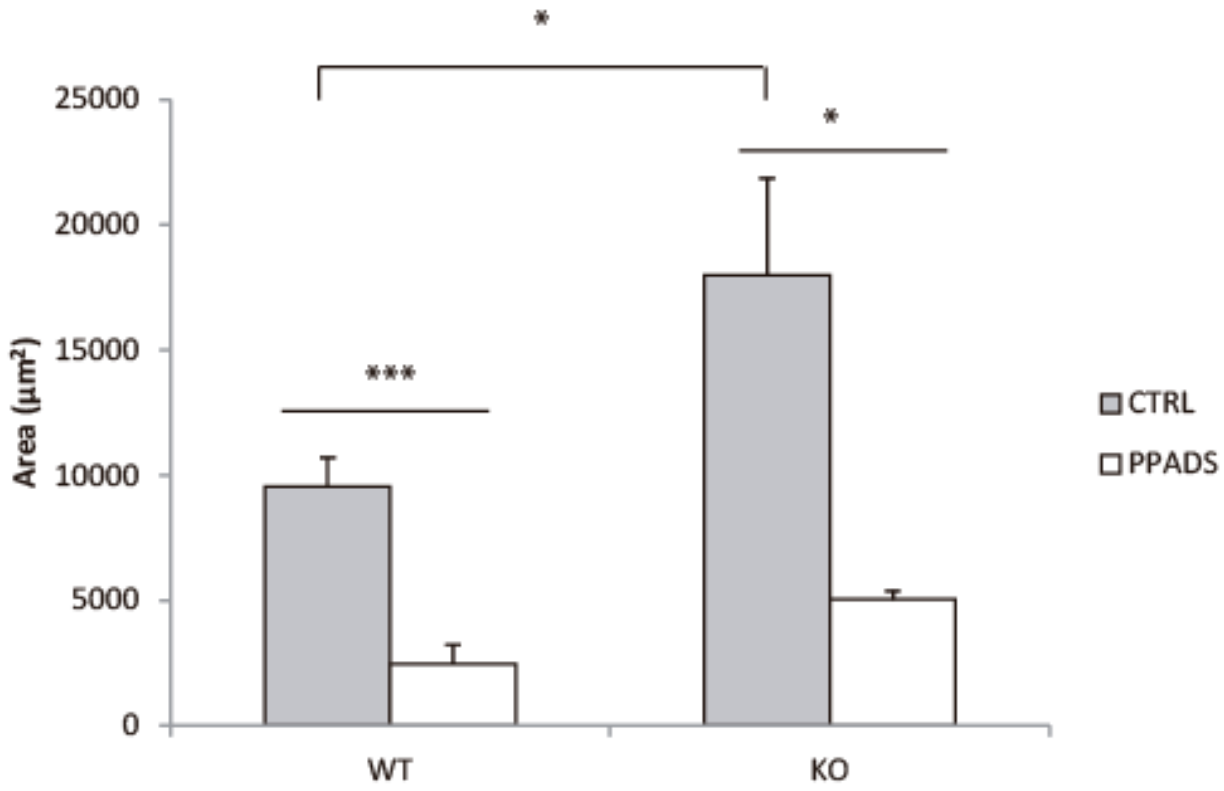

Fig. 4.3 Calcium waves are purine-dependent

Calcium waves are electrically evoked on wild-type and knock-out mice in the presence of PPADS: in both wild-type and knock-out there is a significant decrease of wave spread with PPADS application.

* for P < 0.05, *** for P < 0.001, t-test.

From the previous experiment, both wild-type and knock-out mice are sensitive to a purinergic mechanism. Further experiments aimed at assessing how the purinergic pathway has an influence on the model.

6.2.3. Calcium wave propagation in CD39 $^{-/-}$ mice is rescued by apyrase application

Apyrase is an adenosine 5′ - diphosphatase adenosine 5′ - triphosphatase (*EC 3.6.1.5*) that mimics the dephosphorylation of ATP and ADP to AMP of the CD39 protein. To show proof of function, it was investigated whether apyrase application (10 U mL^{-1}) on acute brain slices in the absence of CD39 would restore its function.

In CD39 $^{+/+}$, the calcium wave spread 6353.44 ± 1441.94 μm^2. This spread was reduced to 4678.34 ± 1617.28 μm^2 with apyrase application, in a non-significant manner (n = 16, P = 0.2).
However, in CD39 $^{-/-}$, the spread of the calcium wave was significantly larger than in wild-type mice (10470.56 ± 1867.33 μm^2, n = 12, P = 0.04) and was reduced with apyrase application (4241.66 ± 1320.36 μm^2, P = 0.008), which was not significantly different from wild-type values (P = 0.17, Fig. 4.4)

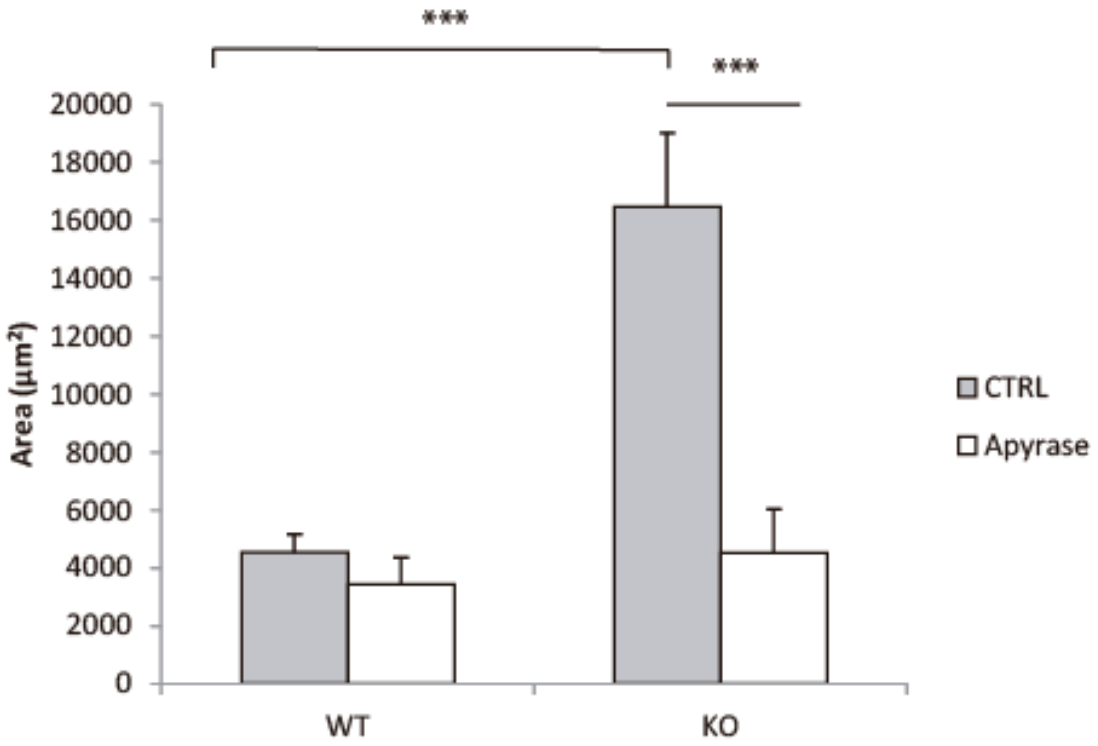

Fig. 4.4 Apyrase application in CD39 knock-out mice restores the wild-type phenotype

Calcium waves are electrically evoked on wild-type and knock-out mice in the presence of apyrase: in the wild-type there is a non-significant decrease, while in the knock-out the calcium wave is significantly reduced.

*** for $P < 0.001$, t-test.

6.2.4. Direct ATP or ARL 67156 application does not mimic CD39 $^{-/-}$ calcium wave behaviour

To mimic the knock-out phenotype pharmacologically, drugs were applied to increase ATP levels in acute brain slices of wild-type mice: namely by direct application of ATP (300 µM) or ARL 67156 (100 µM), an ecto-apyrase inhibitor that prevents dephosphorylation of ATP.

With ARL67156 application, there was a non-significant change from 5480.16 ± 1938.29 µm^2 from control to 4496.08 ± 1802.92 µm^2 with drug application ($n = 6$, $P = 0.6$, Fig. 4.5 A). With ATP application, the values changed from 3724.92 ± 243.68 µm^2 (control) to 2899.58 ± 413.68 µm^2 (ATP), also in a non-significant manner ($n = 6$, $P = 0.4$, Fig. 4.5 B).

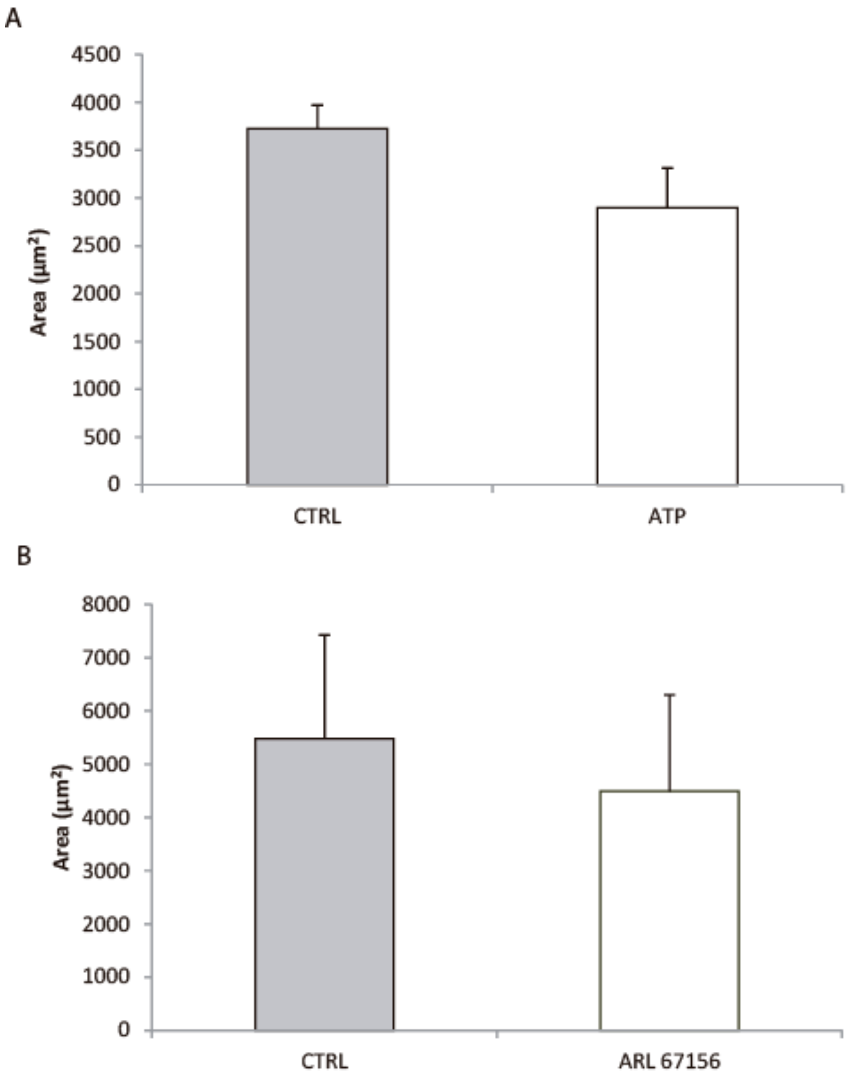

Fig. 4.5 ATP and ARL 67156 application does not affect the calcium wave spread

Calcium waves are electrically evoked on wild-type mice in the presence of ATP (A) and ARL 67156 (B), in both situations there is not a significant change in the calcium wave spread.

6.3. Neurons from CD39 -/- mice have an increased network excitability

The calcium wave experiments illustrate the effect of CD39 on glia cells. To understand how it affects neurons, patch-clamp experiments were performed in the gray matter. The barrel cortex was chosen because it is a well-known neuron-astrocyte interaction study model currently used in the lab (see, for e.g. Benedetti et al., 2011).

6.3.1. Neurons in CD39 knock-out mice are more excitable than in the wild-type

To study the influence of CD39 on neuronal activity, neurons from layer II/III and layer IV from the barrel cortex, in acute brain slices from CD39 $^{+/+}$ and CD39 $^{-/-}$ mice, were patch-clamped at -70 mV and an electrical stimulation was evoked, as previously described (Benedetti et al., 2011).

In CD39 $^{-/-}$, 16 out of 22 neurons showed spontaneous action potentials during the repolarization phase, (1 to 30 action potentials, an average value of 6.8 ± 1.8), that was not observed in wild-type neurons (n = 17, Fig. 4.6 A).

The neurons had a similar average resting potential of -68.7 ± 0.9 mV in wild-type and -70.2 ± 0.5 mV in knock-out mice (P = 0.09). Electrical stimulation evoked a depolarization with an amplitude of 23.13 ± 1.96 mV in wild-type and a significantly larger one of 36.21 ± 2.35 mV in knock-out (STM dep, P = 9.5 x 10^{-5}, Fig. 4.6 B). After the stimulation, the membrane repolarized with a half repolarization time (Half rep, Fig. 4.6 C) of 0.60 ± 0.04 s in wild-type and 0.95 ± 0.35 s in knock-out (P = 0.16). To further quantify the neuronal depolarization, the integral of membrane depolarization over time was quantified (I STM, Fig. 4.6 D): in wild-type, I STM was 24.2 ± 2.2 mV*s, in knock-out it was significantly increased: 53.7 ± 11.6 mV*s (P = 0.01).

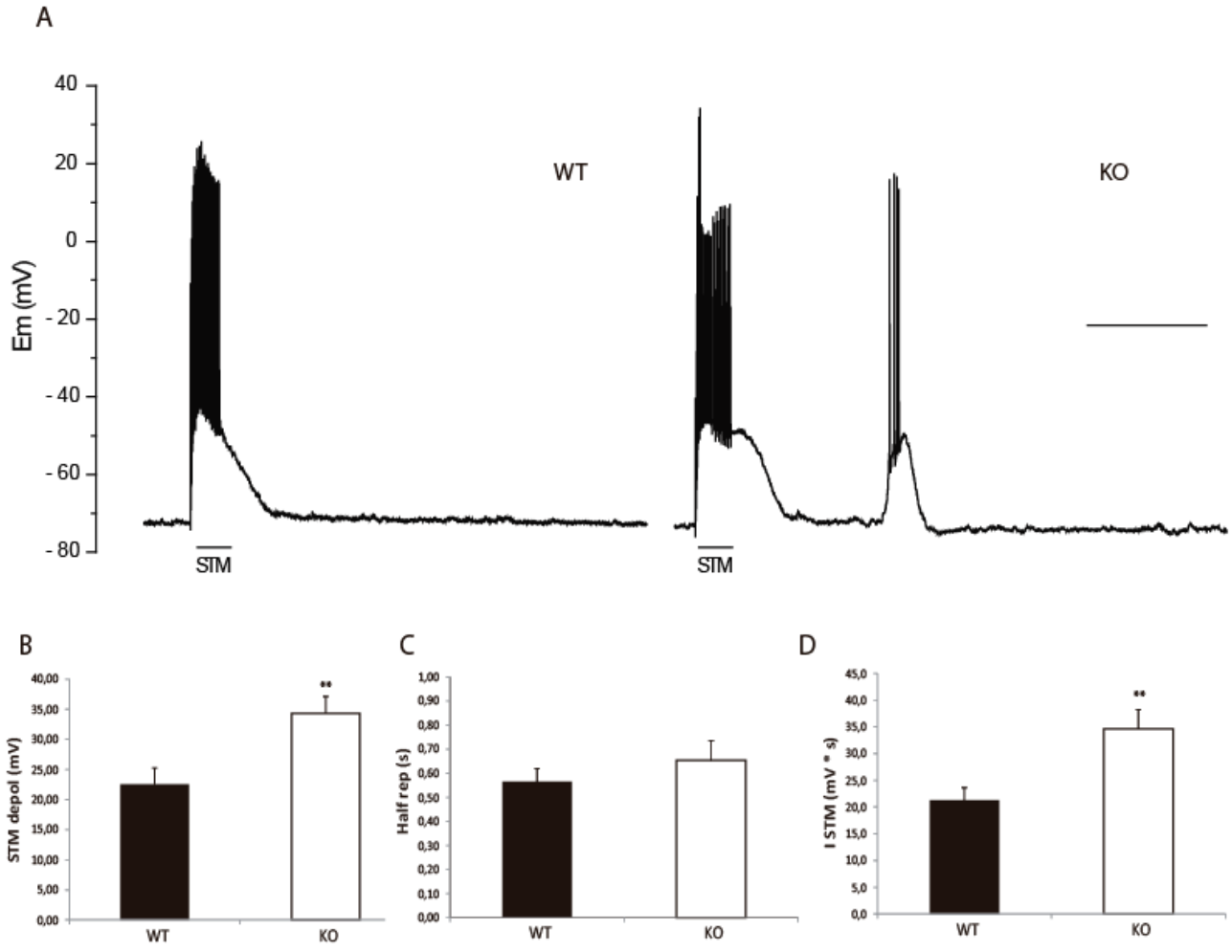

Fig. 4.6 Neurons in knock-out mice show a higher degree of excitability than in the wild-type

(A) Membrane potential (Em) recording from a neuron within the stimulated barrel. Stimulation-evoked neuronal response in wild-type (WT) and in knock-out mice (KO). The stimulation is indicated by bar with STM, bar 1s. (B) Stimulus-evoked depolarization (STM depol), (C) Time for half repolarization (Half rep), (D) Integral of membrane depolarization over time (I STM).

** for $P < 0.01$, t-test.

6.3.2. Frequency of spontaneous excitatory post-synaptic activity is increased in knock-out mice

To further characterize CD39's effect on neurons, the spontaneous excitatory post-synaptic activity was measured during baseline recordings (Fig. 4.7 A). The neurons

were clamped at -70 mV, close to the chloride equilibrium potential, to minimize contributions from inhibitory currents.

The frequency of spontaneous excitatory post synaptic currents (sEPSCs) is significantly increased from 1.0 ± 0.1 Hz in CD39 $^{+/+}$ (n=12) to 2.7 ± 0.4 Hz in CD39 $^{-/-}$ (n=11, P= 0.0001, Fig. 4.7 B). There were no significant changes in the decay constant (7.6 ± 1.3 ms in CD39 $^{+/+}$ and 8.8 ± 1.9 ms in CD39 $^{-/-}$, P = 0.2) and in the amplitude (16.4 ± 0.2 pA in CD39 $^{+/+}$ and 14.2 ± 0.5 pA in CD39 $^{-/-}$, P = 0.1). The neuronal average access resistance (Ra) was 21.1 ± 1.3 MΩ (15 MΩ < Ra < 26 MΩ) for WT and 23.0 ± 0.6 MΩ (18 MΩ < Ra < 27 MΩ) for KO (P = 0.1).

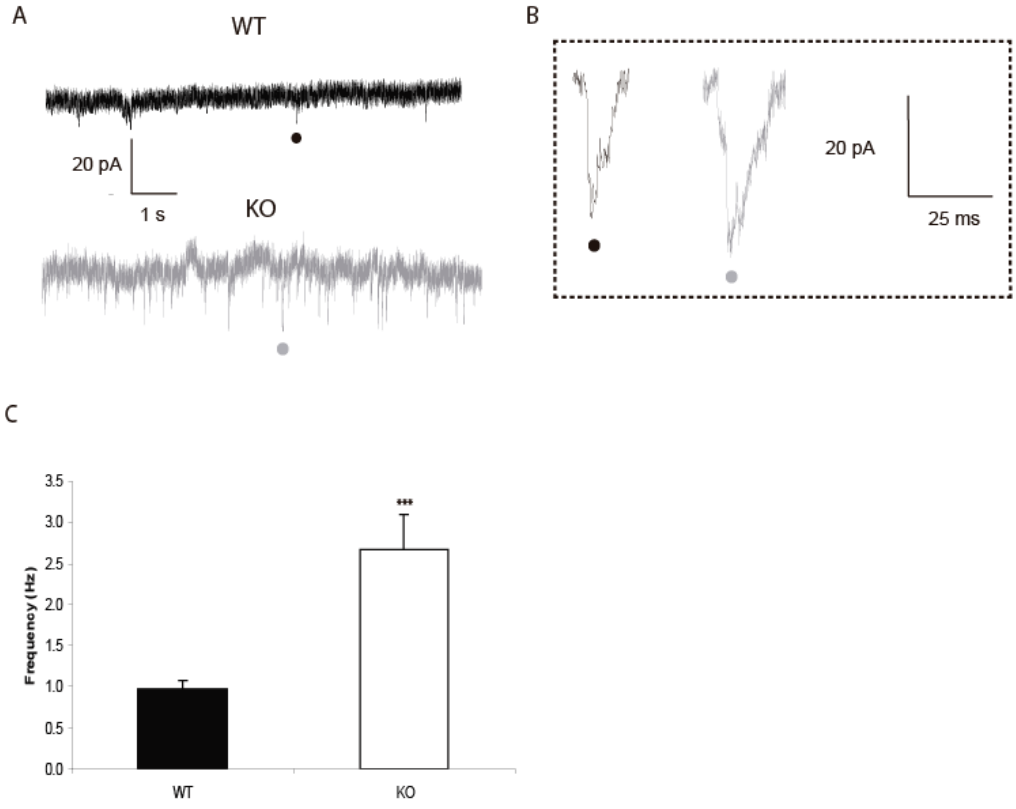

Fig. 4.7 Frequency of spontaneous excitatory post-synaptic events is increased in knock-out mice

(A) Representation of voltage clamp recording in wild-type and knock-out,mice (B) Single events displayed at higher magnification, (C) EPSC frequency is significantly increased in knock-out mice.

*** for P < 0.001, t-test.

6.3.3. PPADS application increases neuronal excitability like CD39 $^{-/-}$

To investigate the influence of the purinergic pathway on neurons, the neuronal evoked response in layer II/III and layer IV barrel neurons in acute brain slices was measured before and after PPADS application to CD39 $^{+/+}$ mice (100 µM).

After PPADS application, all cells showed spontaneous action potentials during the repolarization phase, (1 to 6 action potentials, an average value of 3.8 ± 0.7), that was not observed in control neurons. (n = 11, Fig. 4.8 A).
The resting potential remained unchanged before (- 69.6 ± 0.6 mV) and after drug application (- 68.7 ± 0.7 mV, P = 0.2). PPADS prolonged the time for repolarization (Half rep) from 0.5 ± 0.1 s to 0.9 ± 0.2 s (P = 0.01, Fig. 4.8 B) but did not significantly affect the STM dep (21.49 ± 3.09 mV for control versus 19.44 ± 3.00 mV for PPADS, P = 0.3, Fig. 4.8 C) or I STM (19.1 ± 3.7 mV*s for control versus 26.3 ± 5.7 mV*s, P = 0.2, Fig. 4.8 D).

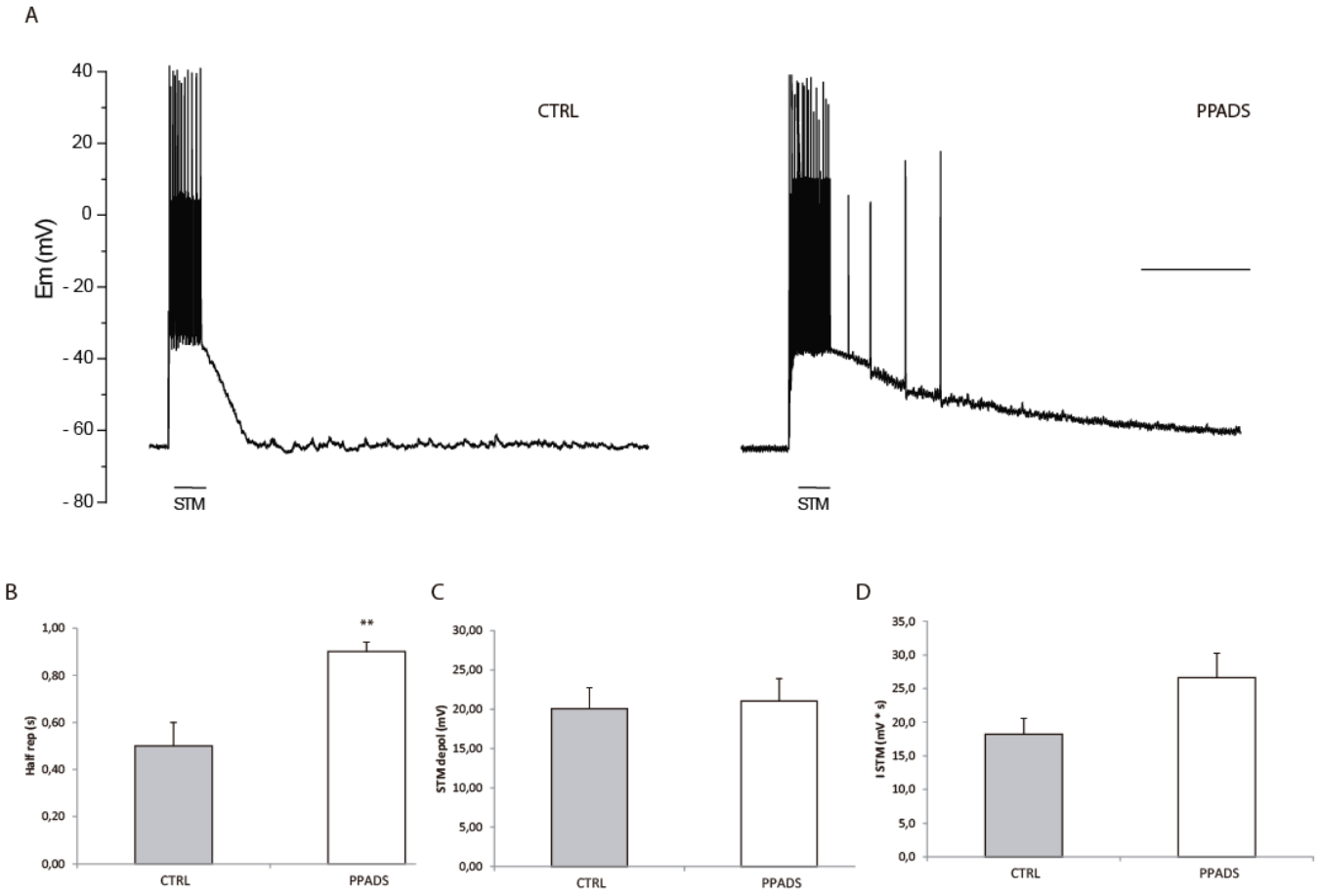

Fig. 4.8 PPADS increases neuronal excitability in wild-type mice

(A) Membrane potential (Em) recording from a neuron within the stimulated barrel. Stimulation-evoked neuronal response before (CTRL) and after PPADS application (PPADS) in wild-type mice. The stimulation is indicated by bar with STM, bar 1s. (B) Time for half repolarization (Half rep), (C) Stimulus-evoked depolarization (STM depol), (D) Integral of membrane depolarization over time (I STM).

** for $P < 0.01$, t-test.

PPADS application induced an increase of spontaneous firings after the electrical stimulation. This increase in neuronal excitability is similar to the one observed in CD39 $^{-/-}$ mice.

6.3.4. Direct ATP or ARL 67156 application does not mimic the increase in neuronal excitability observed in CD39 $^{-/-}$ mice

Similarly to the calcium wave experiments, ATP (300 µM) or ARL67156 (100 µM) were applied to acute brain slices from CD39 $^{+/+}$ mice to mimic the CD39 phenotype (Fig. 4.9).

Both ARL 67156 and ATP application did not induce any significant changes on the neurons, with stimulus-evoked depolarization, half-time for repolarization and integral of response depolarization unchanged from the control situation (n = 6, P > 0.1, Table 11). Additionally, no spontaneous action potentials during the repolarization phase were observed.

	STM depol (mV)		I STM (mV * s)		Half rep (s)	
	Control	Drug	Control	Drug	Control	Drug
ATP	20.11 ± 1.70	21.21 ± 1.34	19.1 ± 0.8	19.6 ± 0.5	0.5 ± 0.2	0.6 ± 0.1
ARL 67156	21.13 ± 1.34	20.99 ± 1.45	17.1 ± 0.7	18.5 ± 0.3	0.6 ± 0.3	0.7 ± 0.2

Table 10. ATP and ARL67156 do not affect neuron evoked depolarization

Values for stimulus-evoked depolarization (STM depol), integral of membrane depolarization over time (I STM) and time for half repolarization (Half rep) for before (Control) and after drug application (Drug).

7. Discussion

Soon after the CD39 $^{-/-}$ mouse model was created (Enjyoji et al., 1999) and CD39 expression was assigned to microglia and vascular endothelial cells (Braun et al., 2000), the authors already speculated that CD39 could regulate P2 receptor-mediated functions of microglia as well as influence nucleotide signalling between neurons or astrocytes that are associated with extensive microglial processes (Braun et al., 2000). CD39 activity is important for microglia in both physiology and pathology, so a study of its effects on a physiological context is quite important to further understand the pathological one (Kettenmann et al., 2011).

Previous studies with the CD39 $^{-/-}$ animal assessed the blood regulation (e.g. Enjyoji et al., 1999) and microglial specific functions (phagocytosis [Bulavina et al., 2013] and migration [Färber et al., 2008]), to name a few.
This is, to our knowledge, the first study of a CD39 $^{-/-}$ mouse focusing on the effects on neuron and astroglial signalling in acute brain slices (there are, for e.g., other studies with neuronal cell cultures, Corti et al., 2011). The work presented here will allow a more in-depth comprehension of microglia regulation of the surrounding environment, as well as highlighting the role of purinergic signalling in its maintenance.

7.1. Nucleotides are metabolized by CD39 present in microglia

CD39 is fundamental in modulating microglia's auto- and paracrine purinergic mechanisms: since it hydrolyses extracellular ATP and ADP rapidly to AMP, it also protects $P2X_1$ and $P2Y_1$ receptors from desensitization, terminates P2 signalling and favours adenosine generation, which ultimately activates P1 pathways (Robson et al., 2006). Fluorescence resonance energy transfer (FRET) studies showed CD39 in close proximity to a number of P2 and P1 receptors, unlike E-NTPDase 2 (Kukulski et al., 2011). These studies further emphasize the importance of CD39 in the control of P2 and P1 receptor activation.

The phosphate assays show that in the absence of CD39, microglia cells are unable to metabolize extracellular ATP and ADP. This CD39 knock-out disruption of the purinergic signalling has consequences for the surrounding environment, which will be discussed further.

7.2. Astrocyte-mediated calcium waves are influenced by CD39

Calcium waves are an astrocyte-evoked phenomenon that spread within the glial network. It has been well-characterized in cell cultures (Haydon, 2001), isolated retina (Newman, 2001), acute brain slices (Schipke et al., 2002) and in the intact living brain (Hoogland et al., 2009).

Calcium wave propagation is explained by two possible mechanisms: (1) ATP is released from astrocytes onto the extracellular space and activates purinergic receptors in neighbouring astrocytes, leading to elevation of internal Ca^{2+} (*long-distance signalling*); and (2) diffusion of $Ins(1,4,5)P_3$ through gap junctions, binding to its receptor and causing the release of Ca^{2+} from internal stores (*short-distance signalling*) (Fig. 1.4 b; Halassa and Haydon, 2010).
Previous studies from our lab show that while both mechanisms co-exist in calcium wave propagation in gray matter, in white matter calcium waves are independent of gap junction coupling and depend solely on the ATP regenerative mechanism. This hypothesis was further corroborated by an observed increase of extracellular ATP levels during the wave propagation (Haas et al., 2006) and an inhibition of the calcium waves after application of a broad spectrum purinergic receptor antagonist (Schipke et al., 2002). Studies from other research groups also reveal this ATP-mediated calcium signalling in white matter astrocytes (James and Butt, 2001; Hamilton et al., 2008).
The *corpus callosum*, as a white matter tract, is the ideal model to study glial-glial interaction, since it is independent from neuronal activity. Indeed, previous studies of evoked calcium waves showed no effect on the wave in the presence of TTX (Schipke et al., 2002). Similarly, ATPase activity was essentially absent in the *corpus callosum*, except for the staining of microglia and microvessels, so CD39 effects can be uniquely investigated (Langer et al., 2008).

In the present study, calcium waves were evoked in the *corpus callosum* of CD39 $^{+/+}$ and CD39 $^{-/-}$ mice. The calcium wave spread significantly further in the knock-out animal, in a purine-dependent mechanism that is inhibited by PPADS application. Furthermore, CD39 is responsible for this difference in wave propagation, since apyrase application to CD39 $^{-/-}$ restored the wild-type phenotype. Attempts to reproduce the CD39 $^{-/-}$ pharmacologically, with direct application of ATP or ARL 67156 (CD39 blocker) were not successful. This illustrates how the changes induced by CD39 deletion have a longer lasting and deeper effect on the animal than just drug application, which has only a limited amount of time to act during the experiment.

Although astrocytic calcium waves are discussed mostly as a mean by which astrocytes influence neuronal signal transmission (e.g., neuronal migration during brain development), they also meet the requirements for a mechanism signalling pathological events in the brain over large distances (Abbracchio and Ceruti, 2006; Koizumi, 2006). There is evidence that glial cells can sense pathologic events, which have occurred hundreds of micrometres away. After brain injury, microglial cells are activated several millimetres away from the lesion site. The calcium wave can be a pathological mechanism to recruit microglia and, indeed, studies show that the astrocytic calcium wave has an effect on microglia (Schipke et al., 2002). In the present study, the normal purinergic signalling in microglia is disrupted by CD39 deletion and is subsequently having an effect on astrocytes.

7.3. Neurons from CD39 $^{-/-}$ mice have an increased network excitability

The previous section described how CD39 has an effect on glia cells. To investigate a possible effect on neurons, the barrel cortex model was used for experiments. Previous work demonstrated that astrocytes discriminate and selectively respond to the activity of a subpopulation of neurons (Schipke et al., 2008). More recently, it has been shown that astrocytes inhibit neuronal activity in a GABA-mediated mechanism (Benedetti et al., 2011).

From Benedetti et al. (2011), when astrocyte-mediated neuronal inhibition is blocked (by dialyzing the astrocytic network with BAPTA, a Ca^{2+} chelator), the neurons showed an increase of excitability. This neuronal excitability is notably characterized by spontaneous firing of action potentials during the repolarization phase, as well as significant changes in the integral of membrane depolarization over time, in time for repolarization and in stimulus-evoked depolarization.

Neurons in the knock-out mouse showed this increase in excitability, unlike the wild-type counterpart. sEPSC frequency was significantly increased in the CD39 $^{-/-}$ mouse, further supporting the hypothesis that CD39 deletion induces an excitatory effect on neurons.
In addition, this neuronal excitability was mimicked upon P2 receptor block with PPADS, indicating that the excitability is indeed purine related. It would seem that purinergic transmission is responsible for the maintenance of neuronal inhibition.
It is possible to speculate that this neuronal inhibition would not be due to ATP, but to its metabolite adenosine, which activates P1 receptors. Adenosine mediated-inhibition can explain why direct application of ATP or ARL 67156 (CD39 blocker), failed to mimic the effect observed in the CD39 knock-out mouse. Direct ATP application would not have a significant effect because it would eventually be metabolized to adenosine; and at the same time, ARL 67156 did not successfully prevent all the ATP conversion to adenosine, due to its insufficient amount and/or experimental time constraints. Both drugs would maintain a normal degree of adenosine-mediated inhibition, unlike the CD39 $^{-/-}$ mouse.

This regulation has been described in other systems, e.g. the hippocampus, where adenosine is involved in the control of heterosynaptic inhibition (Serrano et al., 2006) or indeed the barrel cortex, where thalamic excitation is decreased by adenosine receptor activation (Fontanez and Porter, 2006). Alternatively, there are other regulatory mechanisms, such as stimulation of inhibitory GABAergic interneurons via ATP released from astrocytes, which also results in increased synaptic inhibition in the hippocampus (Bowser and Kakh, 2004).

7.4. Possible model

Though it is not possible at this stage to build a model from the experiments described, it is viable to speculate on a possible mechanism. Future experiments (described further) will later corroborate or disprove the presented model.

7.4.1. Purinergic pathway

To summarize, it seems that the effects observed in neurons and astrocytes due to CD39 deletion are two-fold:

(1) CD39 $^{-/-}$ does not metabolize ATP, which accumulates in the extracellular space: the high levels of ATP activate P2 receptors and their subsequent excitatory effects;

(2) lack of ATP dephosphorylation results in less adenosine production, which in turn decreases P1 activation (via A1 receptors) and decreases adenosine-mediated inhibition

In addition, P1 and P2 negatively regulate each other, strengthening the overall excitatory effect.

7.4.2. Neuron-glia interaction mechanism

The experiments described in neurons and astrocytes point towards a CD39-dependent regulation of neuroglial transmission. Many studies illustrate the bidirectional neuron-astrocyte modulation (e.g. Serrano et al., 2006; Porter and McCarthy, 1996) and indeed some authors claim that gliotransmission is directly dependent on microglia activation (Agulhon et al., 2012), paving the way for a different neuron-glia mechanism (whereas glia refers to astrocyte/microglia).

The evidence suggests that CD39 from microglia has an effect on astrocytes: this is shown by the different behaviour of the calcium wave in the presence and absence of CD39. Since astrocytes and neurons modulate each other, it is possible to suggest a mechanism where (**1**) microglia affects astrocytes, which in turn modulate neurons; or (**2**) microglia affects neurons directly (which relay this modulation towards astrocytes) (Fig. 5.1).

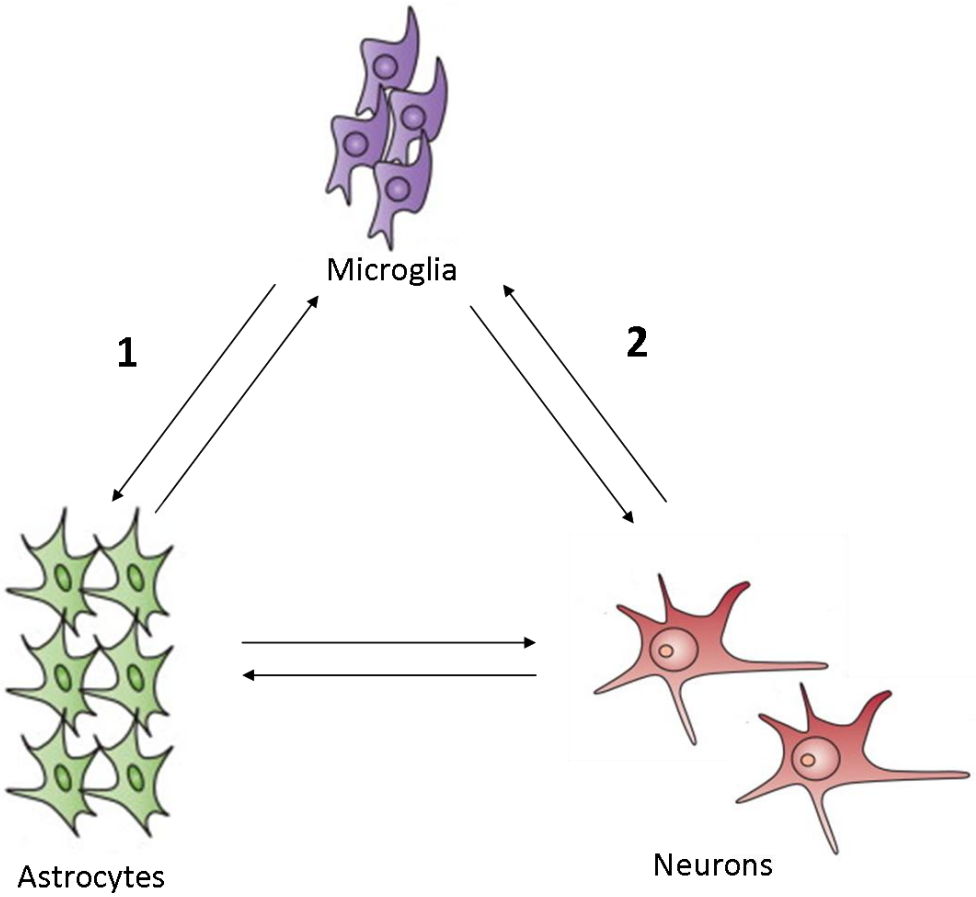

Fig. 5.1 Possible model

Evidence suggests a mechanism where (**1**) microglia affects astrocytes, which in turn modulate neurons in a bidirectional mechanism; or (**2**) microglia affects neurons directly (which relay this modulation towards astrocytes).

Adapted and modified from Philips and Robberecht, 2011.

The mechanism proposed is not entirely new: Pascual and collaborators (2012) proposed that in the hippocampus, microglia are the upstream regulators that modulate neurons via astrocyte regulation. In summary, microglia activation releases ATP which will bind to $P2Y_1$ receptors on the surface of astrocytes. Astrocytes will then release

glutamate which activates neuronal mGluR5 receptors, increasing EPSCs in these cells (Pascual et al., 2012).

Other studies point towards a microglia modulation of neuronal activity via BDNF (Ferrini and De Koninck, 2013) or focus on microglia regulation of active synapses (Ji et al., 2013; Miyamoto et al., 2013). Recent reviews also emphasize microglia's role as a neuronal modulator (Béchade et al., 2013; Eyo and Wu, 2013).

While CD39 is indeed present in the extracellular membrane of endothelial cells lining blood vessels in the brain, they are separated from the rest of the brain by the BBB. Astrocytic endfeet constituting the *glia limitans* surround both pericytes and vascular endothelium, in a tight selective barrier that prevents passage of molecules towards the rest of the brain, with few exceptions. Interestingly, it has been shown that astrocytic endfeet express purinergic receptors $P2Y_2$ and $P2Y_4$ so it could be theorised that CD39 in endothelial cells could influence purinergic signalling in the astrocytic endfeet (Simard et al., 2003). However all three cell types in the BBB – endothelial cells, pericytes and astrocytes – are physically separated from each other by the basal lamina, preventing direct contact between endothelial cells and astrocytes (Abbott et al., 2010; Nico and Ribatti, 2012). Indeed, experiments in which astrocytic endfeet responded strongly to ATP had no significant effect in endothelial cells and pericytes, further corroborating this (Simard et al., 2003).
It can be surmised that while CD39 deletion affects vascular endothelial cell functions, such as blood flow and homeostasis (Enjyoji et al. 1999), it does not have a direct effect on neurons or glia cells. However, indirect contributions from this disrupted thromboregulation are not to be overlooked.

7.5. Future Perspectives

Future experiments were aimed at constructing a model detailing the mechanism by which CD39 regulates neuronal and astrocytical function and its effects on the purinergic signalling in the surrounding environment.

7.5.1. Patch-clamp experiments

EPSCs only show an increase in the frequency of excitatory post-synaptic events, exactly which type of events (NMDA-receptor mediated, etc.) needs to be further investigated with specific receptor blockers.
It would also be interesting to apply apyrase to the knock-out mouse to see if there is a rescue of the wild-type phenotype, akin to what happened with the calcium wave experiments.

7.5.2. End pathway effects

While most excitatory effects observed in the experiments could be ascertained to an excess of extracellular ATP – which is not being degraded due to an absence of CD39 – it is important to remember that that results in lack of inhibitory adenosine.
Indeed, previous experiments with activation of P1 receptors (via application of the non-hydrolysable analog of adenosine NECA), reduce microglia phagocytosis – a P2 dependent mechanism - in both CD39 $^{+/+}$ and CD39 $^{-/-}$ mice (Bulavina et al., 2013). It would be interesting to see if NECA application would rescue the wild-type phenotype in CD39 $^{-/-}$ mice, in both calcium wave and patch-clamp experiments.

The proof of principle for this excitation/inhibition disbalance should show high ATP and low adenosine levels. Accordingly, extracellular ATP levels can be measured with the luciferine/luciferase method (*in vitro*, cell culture and brain slices) (Wieraszko, et al., 1989) and microdialysis in the intact brain followed by HPLC for quantification (*in vivo*) (Hagberg et al., 1987). It is also possible to use, *in vitro* and *in vivo*, commercially available ATP electrodes to determine its concentration (Dale and Frenguelli, 2012).
For adenosine, the same *in vivo* method of microdialysis and subsequent HPLC can be used, and there are also adenosine electrodes commercially available (Dale et al., 2002).

In addition, this ATP/adenosine unbalance would result in differential expression of P1/P2 receptors, therefore it would be interesting to quantify their expression numbers via qPCR and/or microarray analysis.

Furthermore, it would be interesting to identify which purine receptors are involved in the mechanism described, so specific pharmacological studies (application of specific purine receptor antagonists) should be used in both calcium wave and patch-clamp experiments.

7.5.3. Developmental changes I: study performed in young animals

All experiments were done on young (P8-P10) animals, firstly due to the calcium experiments that require a bulk-loading of the calcium indicator Fluo-4 AM, which is harder to do after P14; and secondly due to the highly coupled astrocytic network at this age, which is a good study model for the neuron-astrocyte interaction. However, this restricts the conclusions taken out of this study, since it cannot be applied to constitute a broad model of CD39 behaviour in the CNS. Indeed, preliminary experiments with qPCR (n=3, data not shown) indicate a significant increase of CD39 expression with age, which can indicate a more prominent role of CD39 in adult animals. In the context of development biology, this work is useful to understand the associated changes of microglia function over time and to understand the underlying neuroinflammation mechanism.

7.5.4. Developmental changes II: adult vs. young animals, a difference in modulation?

After the phosphate assays in microglia cell culture (see *4.1.1. Microglia in CD39 $^{-/-}$ mice do not metabolize ATP or ADP (in vitro)*), the same experiment was performed in acute brain slices of young (P8-P10) and adult (over P30) mice. In adult animals (n=9 for WT, n=7 for KO), extracellular ATP and ADP dephosphorylation was significantly

reduced in CD39 $^{-/-}$ mice (P = 0.009 and P = 4.6 x 10^{-5}, respectively), while in the young animal (n=6 for WT and KO) there was no significant change between the wild-type and the knock-out (P = 0.2 for ATP and P = 0.07 for ADP, Fig. 5.2). This result seems to indicate that CD39 does not have a role in purine metabolization in young animals, only in adults.

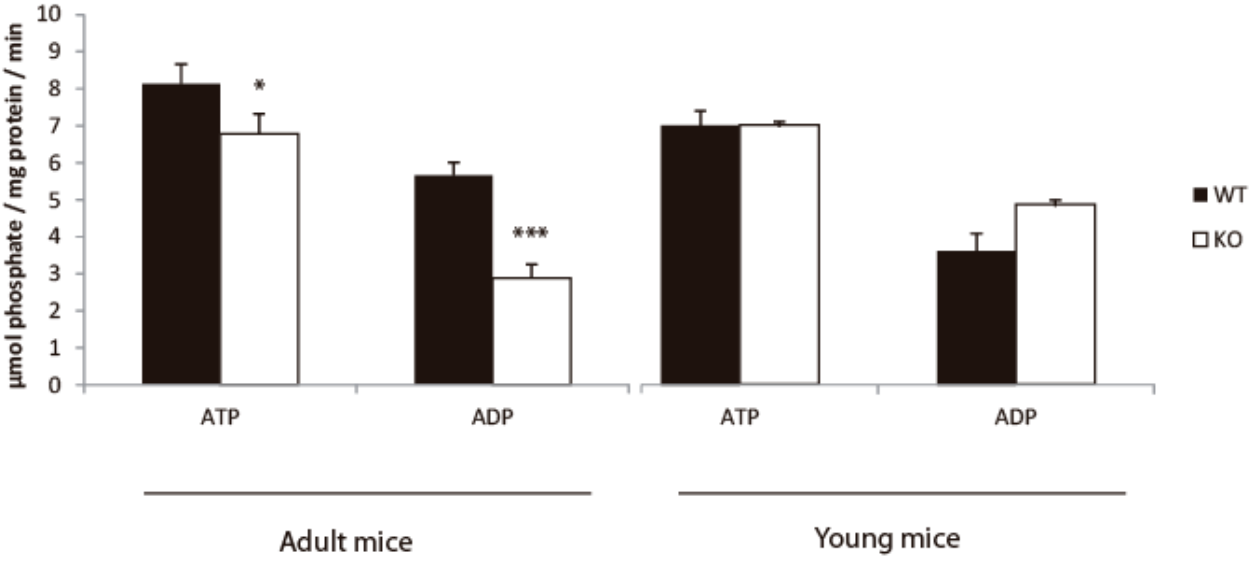

Fig. 5.2 ATP and ADP dephosphorylation is different in young and adult mice

In acute brain slices in adult mice, ATP and ADP are significantly less dephosphorylated in the knock-out than in the wild-type. In young mice, the rate of dephosphorylation is non-significant between wild-type and knock-out.

* for P < 0.05, *** for P < 0.001, t-test.

This result is highly surprising, since all experiments described so far show a specific role for CD39 in nucleotide metabolization in young animals. However, since these experiments are performed in acute brain slices, there are many variables to consider.

Firstly, the model being studied is no longer only composed of microglia cells, so other nucleotidases are involved, such as E-NTPDase 2 from astrocytes.

Secondly, as mentioned before (*5.5.3. Developmental changes I: adult vs. young animals, a difference in modulation?)*, CD39 expression seems to increase with age, which means that in adult animals CD39 would have more overall influence than in young animals, skewing the results. It is important to remember that a phosphate assay in a brain slice does not reflect the physiological environment *in situ*, rather a

summation of extracellular ATP and ADP dephosphorylation by all cells. Indeed, it is possible to speculate that in young animals CD39 and E-NTPDase 2 from astrocytes are equally contributing to the final result; in adults it is the CD39 effect that is predominant.

Finally, it is also necessary to consider that, during phosphate assays, the handling of young acute brain slices was more difficult since they were more fragile and prone to breaking when put in the 96-well plate used for the assay – meaning that the results observed in this experiment maybe do not reflect the brain environment in the young animal, but rather a pathophysiological situation.

Taking all this information into consideration, it seems that the phosphate assay in acute brain slices is not the more correct way to assess CD39 activity. The best way would be to assess it indirectly: measuring the amount of extracellular ATP produced in the brain of animals of different ages. For that, ATP levels could be measured with microdialysis in the intact brain followed by HPLC for quantification (Hagberg et al., 1987) and commercially available ATP electrodes to determine its concentration are also an option (Dale and Frenguelli, 2012).

8. References

Abbott, N.J., Patabendige, A. a K., Dolman, D.E.M., Yusof, S.R., and Begley, D.J. (2010). Structure and function of the blood-brain barrier. Neurobiol. Dis. *37*: 13–25.

Abbracchio, M.P., Burnstock, G., Verkhratsky, A., and Zimmermann, H. (2009). Purinergic signalling in the nervous system: an overview. Trends Neurosci. *32*: 19–29.

Abbracchio, M.P., and Ceruti, S. (2006). Roles of P2 receptors in glial cells: focus on astrocytes. Purinergic Signal. *2*: 595–604.

Agmon, A., and Connors, B.W. (1991). Thalamocortical responses of mouse somatosensory (barrel) cortex in vitro. Neuroscience *41*: 365–379.

Agulhon, C., Sun, M.-Y., Murphy, T., Myers, T., Lauderdale, K., and Fiacco, T. A. (2012). Calcium Signaling and Gliotransmission in Normal vs. Reactive Astrocytes. Front. Pharmacol. *3*: 139.

Béchade, C., Cantaut-Belarif, Y., and Bessis, A. (2013). Microglial control of neuronal activity. Front. Cell. Neurosci. *7*: 32.

Benedetti, B., Matyash, V., and Kettenmann, H. (2011). Astrocytes control GABAergic inhibition of neurons in the mouse barrel cortex. J. Physiol. *589*: 1159–72.

Bowser, D.N., and Khakh, B.S. (2004). ATP excites interneurons and astrocytes to increase synaptic inhibition in neuronal networks. J. Neurosci. *24*: 8606–20.

Braun, N., Sévigny, J., Robson, S.C., Enjyoji, K., Guckelberger, O., Hammer, K., Di Virgilio, F., Zimmermann, H. (2000). Assignment of ecto-nucleoside triphosphate diphosphohydrolase-1/cd39 expression to microglia and vasculature of the brain. Eur. J. Neurosci. *12*: 4357–4366.

Bulavina, L., Szulzewsky, F., Rocha, A., Krabbe, G., Robson, S.C., Matyash, V., Kettenmann, H. (2013). NTPDase1 activity attenuates microglial phagocytosis. Purinergic Signal. *9*: 199–205.

Burnstock, G. (2007). Physiology and pathophysiology of purinergic neurotransmission. Physiol. Rev. *87*: 659–797.

Corti, F., Olson, K.E., Marcus, A.J., and Levi, R. (2011). The expression level of ecto-NTP diphosphohydrolase1/CD39 modulates exocytotic and ischemic release of neurotransmitters in a cellular model of sympathetic neurons. J. Pharmacol. Exp. Ther. *337*: 524–32.

Dale, N., and Frenguelli, B.G. (2012). Measurement of purine release with microelectrode biosensors. Purinergic Signal. *8*: 27–40.

Dale, N., Gourine, A. V, Llaudet, E., Bulmer, D., Thomas, T., and Spyer, K.M. (2002). Rapid adenosine release in the nucleus tractus solitarii during defence response in rats: real-time measurement in vivo. J. Physiol. *544*: 149–160.

Daré, E., Schulte, G., Karovic, O., Hammarberg, C., and Fredholm, B.B. (2007). Modulation of glial cell functions by adenosine receptors. Physiol. Behav. *92*: 15–20.

Enjyoji, K., Sévigny, J., Lin, Y., Frenette, P.S., Christie, P.D., Esch, J.S., Imai, M., Edelberg, J. M., Rayburn, H., Lech, M., Beeler, D.L., Csizmadia, E., Wagner, D.D., Robson, S.C., Rosenberg, R.D. (1999). Targeted disruption of cd39/ATP diphosphohydrolase results in disordered hemostasis and thromboregulation. Nat. Med. *5*: 1010–7.

Eyo, U.B., and Wu, L.-J. (2013). Bidirectional Microglia-Neuron Communication in the Healthy Brain. Neural Plast. *2013*: 456857.

Färber, K., Markworth, S., Pannasch, U., Nolte, C., Prinz, V., Kronenberg, G., Gertz, K., Endres, M., Bechmann, I., Enjyoji, K., Robson, S.C., Kettenmann, H. (2008). The Ectonucleotidase cd39 / ENTPDase1 Modulates Purinergic-Mediated Microglial Migration. Glia *341*: 331–341.

Ferrini, F., and Koninck, Y. De (2013). Microglia Control Neuronal Network Excitability via BDNF Signalling. Neural Plast. *2013*: 429815.

Fontanez, D.E., and Porter, J.T. (2006). Adenosine A1 receptors decrease thalamic excitation of inhibitory and excitatory neurons in the barrel cortex. Neuroscience *137*: 1177–84.

Fox, K. (2008). Barrel Cortex (Cambridge University Press, New York, USA).

Haas, B., Schipke, C.G., Peters, O., Söhl, G., Willecke, K., and Kettenmann, H. (2006). Activity-dependent ATP-waves in the mouse neocortex are independent from astrocytic calcium waves. Cereb. Cortex *16*: 237–46.

Hagberg, H., Andersson, P., Lacarewicz, J., Jacobson, I., Butcher, S., and Sandberg, M. (1987). Extracellular adenosine, inosine, hypoxanthine, and xanthine in relation to tissue nucleotides and purines in rat striatum during transient ischemia. J. Neurochem. *49*: 227–31.

Halassa, M.M., Fellin, T., and Haydon, P.G. (2007). The tripartite synapse: roles for gliotransmission in health and disease. Trends Mol. Med. *13*: 54–63.

Halassa, M.M., Fellin, T., and Haydon, P.G. (2009). Tripartite synapses: roles for astrocytic purines in the control of synaptic physiology and behavior. Neuropharmacology *57*: 343–6.

Halassa, M.M., and Haydon, P.G. (2010). Integrated brain circuits: astrocytic networks modulate neuronal activity and behavior. Annu. Rev. Physiol. *72*: 335–55.

Hamilton, N., Vayro, S., Kirchhoff, F., Verkhratsky, A., Robbins, J., Gorecki, D.C., Butt, A.M. (2008). Mechanisms of ATP- and glutamate-mediated calcium signaling in white matter astrocytes. Glia *56*: 734–49.

Hanisch, U.-K., and Kettenmann, H. (2007). Microglia: active sensor and versatile effector cells in the normal and pathologic brain. Nat. Neurosci. *10*: 1387–94.

Hoogland, T.M., Kuhn, B., Göbel, W., Huang, W., Nakai, J., Helmchen, F., Flint, J., Wang, S. S.-H. (2009). Radially expanding transglial calcium waves in the intact cerebellum. Proc. Natl. Acad. Sci. U. S. A. *106*: 3496–501.

James, G., and Butt, A.M. (2001). P2X and P2Y purinoreceptors mediate ATP-evoked calcium signalling in optic nerve glia in situ. Cell Calcium *30*: 251–9.

Ji, K., Akgul, G., Wollmuth, L.P., and Tsirka, S.E. (2013). Microglia actively regulate the number of functional synapses. PLoS One *8*: e56293.

Junger, W.G. (2011). Immune cell regulation by autocrine purinergic signalling. Nat. Rev. Immunol. *11*: 201–12.

Kettenmann, H., Hanisch, U.-K., Noda, M., and Verkhratsky, A. (2011). Physiology of microglia. Physiol. Rev. *91*: 461–553.

Koizumi, S. (2010). Synchronization of Ca2+ oscillations: involvement of ATP release in astrocytes. FEBS J. *277*: 286–92.

Köles, L., Leichsenring, A., Rubini, P., and Illes, P. (2011). P2 receptor signaling in neurons and glial cells of the central nervous system. Adv. Pharmacol. *61*: 441–93.

Kukulski, F., Lévesque, S. a, and Sévigny, J. (2011). Impact of ectoenzymes on p2 and p1 receptor signaling.

Kukulski, F., Lévesque, S.A., Lavoie, E.G., Lecka, J., Bigonnesse, F., Knowles, A.F., Robson, S.C., Kirley, T.L., Sévigny, J. (2005). Comparative hydrolysis of P2 receptor agonists by NTPDases 1, 2, 3 and 8. Purinergic Signal. *1*: 193–204.

Langer, D., Hammer, K., Koszalka, P., Schrader, J., Robson, S.C., and Zimmermann, H. (2008). Distribution of ectonucleotidases in the rodent brain revisited. Cell Tissue Res. *334*: 199–217.

Miyamoto, A., Wake, H., Moorhouse, A.J., and Nabekura, J. (2013). Microglia and synapse interactions: fine tuning neural circuits and candidate molecules. Front. Cell. Neurosci. *7*: 70.

Navarrete, M., Perea, G., Maglio, L., Pastor, J., García de Sola, R., and Araque, A. (2013). Astrocyte calcium signal and gliotransmission in human brain tissue. Cereb. Cortex *23*: 1240–6.

Newman, E.A. (2001). Propagation of intercellular calcium waves in retinal astrocytes and Müller cells. J. Neurosci. *21*: 2215–23.

Nico, B., and Ribatti, D. (2012). Morphofunctional aspects of the blood-brain barrier. Curr. Drug Metab. *13*: 50–60.

Pascual, O., Achour, S. Ben, Rostaing, P., Triller, A., and Bessis, A. (2012). Microglia activation triggers astrocyte-mediated modulation of excitatory neurotransmission. Proc. Natl. Acad. Sci. U. S. A. *109*: E197–205.

Philips, T., and Robberecht, W. (2011). Neuroinflammation in amyotrophic lateral sclerosis: role of glial activation in motor neuron disease. Lancet Neurol. *10*: 253–63.

Porter, J.T., and McCarthy, K.D. (1996). Hippocampal astrocytes in situ respond to glutamate released from synaptic terminals. J. Neurosci. *16*: 5073–81.

Robson, S.C., Sévigny, J., and Zimmermann, H. (2006). The E-NTPDase family of ectonucleotidases: Structure function relationships and pathophysiological significance. Purinergic Signal. *2*: 409–30.

Schipke, C.G., Boucsein, C., Ohlemeyer, C., Kirchhoff, F., and Kettenmann, H. (2002). Astrocyte Ca2+ waves trigger responses in microglial cells in brain slices. FASEB J. *16*: 255–7.

Schipke, C.G., Haas, B., and Kettenmann, H. (2008). Astrocytes discriminate and selectively respond to the activity of a subpopulation of neurons within the barrel cortex. Cereb. Cortex *18*: 2450–9.

Serrano, A., Haddjeri, N., Lacaille, J.-C., and Robitaille, R. (2006). GABAergic network activation of glial cells underlies hippocampal heterosynaptic depression. J. Neurosci. *26*: 5370–82.

Simard, M., Arcuino, G., Takano, T., Liu, Q.S., and Nedergaard, M. (2003). Signaling at the gliovascular interface. J. Neurosci. *23*: 9254–62.

Verderio, C., and Matteoli, M. (2001). ATP mediates calcium signaling between astrocytes and microglial cells: modulation by IFN-gamma. J. Immunol. *166*: 6383–91.

Verkhratsky, A., Krishtal, O.A., and Burnstock, G. (2009). Purinoceptors on neuroglia. Mol. Neurobiol. *39*: 190–208.

Wang, X., Lou, N., Xu, Q., Tian, G.-F., Peng, W.G., Han, X., Kang, J., Takano, T., Nedergaard, M. (2006). Astrocytic Ca2+ signaling evoked by sensory stimulation in vivo. Nat. Neurosci. *9*: 816–23.

Wieraszko, A., Goldsmith, G., and Seyfried, T.N. (1989). Stimulation-dependent release of adenosine triphosphate from hippocampal slices. Brain Res. *485*: 244–250.

Yang, R., and Liang, B.T. (2012). Cardiac P2X(4) receptors: targets in ischemia and heart failure? Circ. Res. *111*: 397–401.

10. Affidavit

Affidavit

“I, Adriana Rocha certify under penalty of perjury by my own signature that I have submitted the thesis on the topic *E-NTPDase 1 modulation of neuronal and astrocytic activity in the CNS* I wrote this thesis independently and without assistance from third parties, I used no other aids than the listed sources and resources.

All points based literally or in spirit on publications or presentations of other authors are, as such, in proper citations (see "uniform requirements for manuscripts (URM)" the ICMJE www.icmje.org) indicated. The sections on methodology (in particular practical work, laboratory requirements, statistical processing) and results (in particular images, graphics and tables) correspond to the URM (s.o) and are answered by me. My interest in any publications to this dissertation correspond to those that are specified in the following joint declaration with the responsible person and supervisor. All publications resulting from this thesis and which I am author correspond to the URM (see above) and I am solely responsible.

The importance of this affidavit and the criminal consequences of a false affidavit (section 156,161 of the Criminal Code) are known to me and I understand the rights and responsibilities stated therein.

Date Signature

11. Appendix

11.1. CV

Mein Lebenslauf wird aus datenschutzrechtlichen Gründen in der elektronischen Version meiner Arbeit nicht veröffentlicht.

9. Acknowledgements

First and foremost I would like to thank Professor Helmut Kettenmann for allowing me to do my doctorate work in his lab in the MDC and for teaching me so much about science and research.

I would like to thank the GABBA program (Graduate Program in the Areas of Basic and Applied Sciences) and its coordinators, Professora Maria de Sousa and Professor Alexandre do Carmo, for choosing me to take part in such a challenging graduate program and for their constant support. Accordingly, I want to acknowledge the FCT funding that supported my work from 2009 to 2012 (SFRH / BD / 33542 / 2008).

Additionally, I want to thank the International Medical Neurosciences Program from the Charité Universitätsmedizin in Berlin, that I was fortunate to integrate from October 2009 onwards.

In the Kettenmann lab, I was fortunate to have the scientific supervision and guidance of Dr Vitali Matyash, who supported me throughout my PhD with helpful discussion, and Dr Bruno Benedetti, who taught me all the main techniques in electrophysiology and always had time for my questions and scientific discussion.
I would also like to mention Dr Ignacio Delgado, with his amazing insights into statistics and programming that helped so much into understanding the data and thinking of new approaches to my project. Dr René Jüttner was invaluable in teaching me the neuronal electrophysiology component of my work and always had free time for my questions, for which I am very grateful. I am also indebted to Dr Susanne Wolf, for her review of this work and her helpful suggestions, now and throughout my work in the lab. Also invaluable were the tips and handy suggestions from Dr Christiane Nolte and Dr Marina Matyash.

I want to thank my lab colleagues Dr Larisa Bulavina, who herself was researching the CD39 function in microglial phagocytosis and gave me the first insights into the project, and Petya Georgieva, who is currently investigating the role of CD39 in inflammation

and who was not only a partner in ideas and brainstorming, but also an invaluable reviewer of this dissertation. I also want to mention the warmth and support from Dr Kristin Stock, Dr Anika Langenfurth, Dr MinChi Ku, Dr Katyani Vinnakota, Nadine Richter, Magdalena Steiner and Daniele Mattei. I am very grateful for all the wonderful times inside and outside the lab.

Also, this work would not have been possible without the excellent technical help from Regina Piske, Nadine Scharek, Hanna Schmidt, Irene Haupt and Michaela Seeger-Zografakis.

I have a special thanks for Birgit Jarchow, who was invaluable in assisting me with all the technical and administrative issues I encountered in Berlin.

Lastly, my very special thanks to all the friends who made my experience in Berlin so much richer and more enjoyable, in particular to Maliha Shah, Sonja Winkler, Jan Walcher, Anne-Kathrin Neuhauβ, Sophia Raphaeline, Nora Schulz, Patrick Sydow, Ella Sylz and Tunc Askan.